



Assessment of Coastal Erosion and Future Projections for North Cove, Pacific County

Authors: Bobbak Talebi, George M. Kaminsky, Peter Ruggiero,
Michael Levkowitz, Jessica McGrath, Katy Serafin, Diana McCandless

This page intentionally left blank



this document was funded in part through a cooperative agreement with the National Oceanic and Atmospheric Administration with funds appropriated for the Coastal Zone Management Act of 1972 through a grant to the Washington Department of Ecology. The views expressed herein are those of the authors and do not reflect the views of NOAA or any of its sub-agencies.



Washington's federal management responsibilities come from the Coastal Zone Management Act, passed in 1972. The act creates a voluntary state-federal partnership between states and NOAA's Office for Coastal Management. The program is administered by the Department of Ecology's Shorelands and Environmental Assistance Program (SEA).

This report is available on the Department of Ecology's website at
<http://www.ecy.wa.gov/programs/sea/czm/Grants.html>
<http://www.ecy.wa.gov/programs/sea/czm/309-improv.html>
<http://fortress.wa.gov.ecy/publications/summarypages1706010.html>

For more information contact:

Bobbak Talebi
Coastal Planner
Shorelands & Environmental Assistance Program
P.O. Box 47600
Olympia, WA 98504-7600
Bobbak.Talebi@ecy.wa.gov
360-407-6529

Washington State Department of Ecology - www.ecy.wa.gov

- | | |
|---------------------------------------|--------------|
| ○ Headquarters, Olympia | 360-407-6000 |
| ○ Northwest Regional Office, Bellevue | 425-649-7000 |
| ○ Southwest Regional Office, Olympia | 360-407-6300 |
| ○ Central Regional Office, Yakima | 509-575-2490 |
| ○ Eastern Regional Office, Spokane | 509-329-3400 |

To request ADA accommodation for disabilities, or printed materials in a format for the visually impaired, call Shorelands and Environmental Assistance Program at Ecology, 360-407-6600. Persons with impaired hearing may call Washington Relay Service at 711. Persons with speech disability may call TTY at 877-833-6341

This page intentionally left blank

Table of Contents

Background	1
Erosion Projections.....	4
Transposed Reference Frame Technique.....	4
Extreme Water Levels	14
Erosion Assessment	19
Appendices	29
Appendix A – Past Shoreline Changes and Estimated Future Shorelines (1971)	29
Appendix B – Shoreline Predictions with +/- One Standard Deviation Uncertainty	30

Background



Figure 1: Left – The North Cove study area and the segment of North Willapa Bay shoreline subject to long-term coastal erosion (a segment known as Washaway Beach). Right – Geographic location of Study in relation to Willapa Bay.

Since 1852, when the U.S. Coast Survey first mapped Willapa (then Shoalwater) Bay, the shorelines, shoals, and entrance channel positions have substantially changed.¹ Between 1852 and 1871, land area grew significantly which was favorable for development. The North Cove community was established in 1884² on the North Willapa Bay shoreline. By 1962, the community grew to 766 parcels within its two subdivisions: Seamobile and Blue Pacific Shores.³ Approximately 340 parcels were created later within three additional subdivisions: Danielson's Tracks, Sea Breeze, and the cranberry fields.⁴ Over the course of the last century shoreline erosion has erased much of what originally existed, particularly along a stretch of shoreline appropriately referred to as Washaway Beach. The North Cove name is now applied to the surrounding community of cranberry farms, resort businesses, and beach homes, which are spread along the landscape from Grayland to Tokeland.⁵

A comprehensive study conducted by the U.S. Army Corps of Engineers (USACE) in 1971, provides the most current characterization of contributing causes for erosion experienced in North Cove. The study found that shoreline retreat is attributed to a cycle (approximately 13 to 20 years) of northward migration of the natural, deep-water entrance channel (the main channel for tidal exchange).⁶ Past shoreline changes and estimated future shorelines were



Figure 2: Left – Google Earth image of the segment of North Cove called Washaway Beach taken in June 1990. Right – Google Earth image of Washaway Beach taken in August 2016.

included in the report (Appendix A). However, the mouth of Willapa Bay is one of the more dynamic, high-energy systems along the coast – shaped by complex regional coastal processes such as waves, tidal flow, circulation, sediment transport, coastal geology and geomorphology. The area is a unique confluence of these interacting physical conditions that remain only somewhat understood.

Erosion has had devastating consequences for North Cove. This area continues to experience the most rapid rates of erosion on the US Pacific Coast – averaging roughly 100 feet per year for the last century.⁷ As reported in 1971, erosion destroyed about 3,000 acres of public and private lands and recreational beaches, including 30 homes, businesses, a grange hall, a public schoolhouse, a Coast Guard Station and has twice forced relocation of the Coast Guard Lighthouse.⁸ A national wildlife refuge was lost in the 1990's.⁹ As of May 2015, approximately 640 of the original 766 parcels within the Blue Pacific Shores and Seamobile subdivisions have succumbed to the eroding shoreline at Washaway Beach, as shown in Figure 3.ⁱ On average, 12 parcels were lost per year over the last 53 years. Many of the parcels were either undeveloped or used exclusively for mobile homes or trailers. However, between 1961 and 1998, at least 161 permanent structures were lost to the marine environment.ⁱⁱ Of the parcels that remain behind the shoreline, fewer than one-third are owned by residents permanently residing in North Cove.^{iii, iv}

ⁱ Numbers based on researcher's visits to the site and quantitative analysis using plotted area maps, Google Earth, and the Pacific County Assessor's Office Mapsifter database.

ⁱⁱ Calculations done by searching Washington State Archives. Since 1998, records are not kept at the State Archives building, but at the local Assessor's office. The Assessor's office does not have the data organized post-1998.

ⁱⁱⁱ Due to the lack of existing information, these numbers are based on approximations determined by information provided by the Pacific County Assessor's Office and the researcher.

^{iv} Determination of primary or secondary resident properties within the study area was done with help by the Assessor's office and cross-referenced with Grayland's associated 98547 zip code

While a long history of previous attempts have been unsuccessful at preventing the ongoing loss of existing development, the search for solutions continues. Reliable data and information on erosion rates provides the basis for understanding risk and evaluating alternative approaches. Updated erosion projections for North Cove are essential to progress.

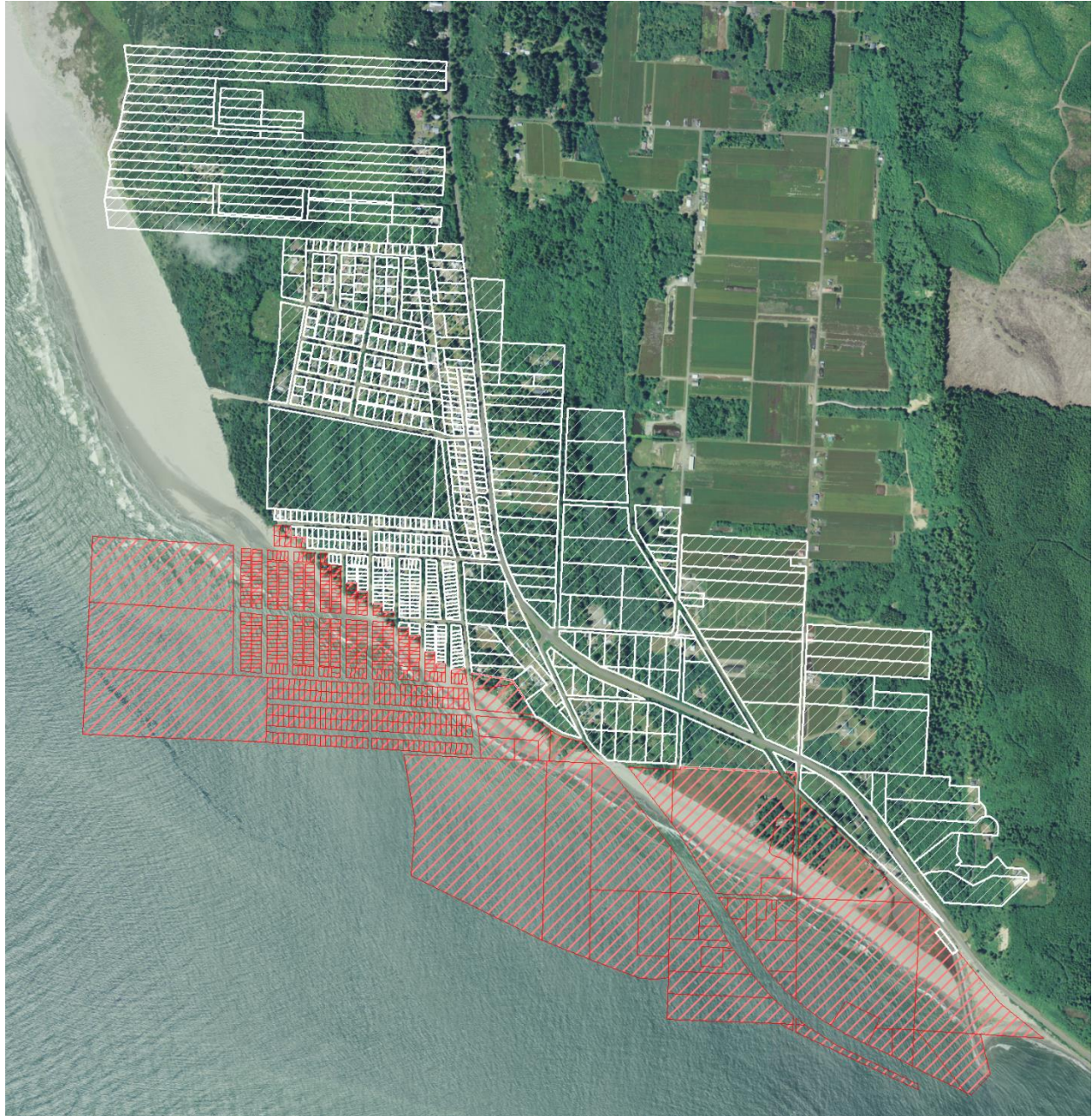


Figure 3: Map of Parcels from the Pacific County Assessor's Office; Red parcels have lost at least 50% of land mass to shoreline erosion as of May, 2015.

In 2013, Ecology received additional financial support from NOAA's Office for Coastal Management to increase understanding of coastal hazard vulnerability and strengthen local capacity to improve coastal resilience in Southwest Washington. While numerous communities

expressed interest and need for further state assistance, North Cove was a high priority. Once selected, Ecology worked with Pacific County's Planning and Community Development Departments to design a project that addressed critical information gaps.

The goal of this report is to raise public awareness of the challenges in erosion management and provide the baseline information necessary to explore alternative options with Pacific County to address future loss.

Erosion Projections

Due to the rapid change in shoreline position, the extended time that had passed since the last studies, and the availability of new scientific methods, project funding was dedicated to new research that would offer a better basis for decision making. More specifically, the Washington Department of Ecology's Coastal Monitoring & Analysis Program (CMAP) worked in partnership with Oregon State University to provide an assessment of coastal erosion and a projection of future erosion rates. The methods for this approach included Transposed Reference Frame Technique in conjunction with Extreme Water Levels, which ultimately produced robust projections of the future shoreline position rooted both in historical changes and the best available understanding of the effects of total water levels and wave runup on erosion. The use of both these methods helps validate and increase confidence in the projections.

Transposed Reference Frame Technique

CMAP analyzed shoreline erosion trends derived from historical shoreline positions from the late 1800s to the present to extrapolate the future potential for erosion. CMAP performed detailed historical change analysis based on trends and statistics to make a projection of the shoreline position at a time horizon defined by the Pacific County Planning Department.

Figure 4 shows a selection of the historical shorelines used in this study and reveals the massive amount of erosion of the area since 1871.

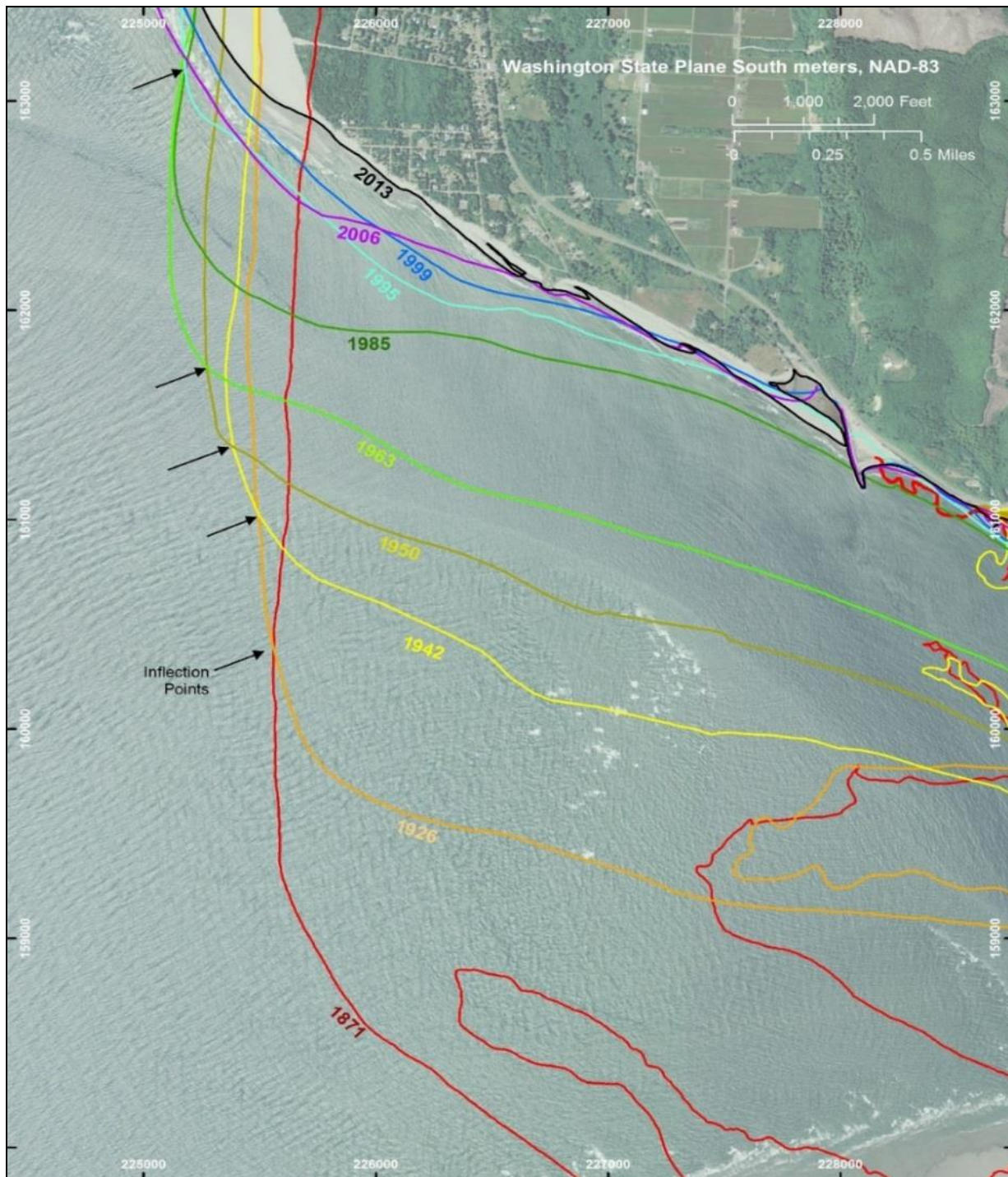


Figure 4: Map showing historical shoreline change along the northern entrance to Willapa Bay. The black arrows indicate inflection points between shoreline retreat toward the southeast and shoreline advance toward the north between consecutive shorelines. The importance of the inflection points are discussed in the following text.

Table 1 shows the 20 historical shorelines digitized using sources and methods described in Kaminsky et al. (1999 and 2010).^{10, 11}

Type of Dataset	Year	Source
T-Sheet	1871	U.S. Coast & Geodetic Survey
T-Sheet	1911	U.S. Coast Survey T-sheet
T-Sheet	1926	NOS T-sheet
Aerial Photo	1942	U.S. Army
Aerial Photo	1945	U.S. Army Corps of Engineers (USACE)
T-Sheet	1950	NOS T-sheet
Aerial Photo	1963	WADNR
Aerial Photo	1970	WADNR
Aerial Photo	1974	WADNR
Aerial Photo	1985	USACE
Aerial Photo	1990	Walker & Associates / USACE
Aerial Photo	1995	NOAA
Aerial Photo	1996	USACE
Aerial Photo	1997	USACE
Aerial Photo	1999	WADNR
Aerial Photo	2001	Spencer B. Gross
Aerial Photo	2006	National Agricultural Imagery Program
Aerial Photo	2009	National Agricultural Imagery Program
Aerial Photo	2011	National Agricultural Imagery Program
Aerial Photo	2013	National Agricultural Imagery Program

Table 1: List of historical shorelines digitized for use in this study.

The area of interest for this study extends from the SR-105 groin along the northern entrance to Willapa Bay to the Pacific County line at Cranberry Beach Road. Throughout this area, historical shoreline change was analyzed at a series of cross-shore transects shown in Figure 5. These transects were drawn to be generally perpendicular to the historical shorelines, centered on the 1963 shoreline, which represented a middle value of the historical datasets (spanning from 1871 to 2013) with similar shoreline orientation. Transects are spaced at roughly 200-meter intervals (+/- 100 meters) alongshore and positioned to minimize their intersection with sharp changes in orientation of the historical shorelines.

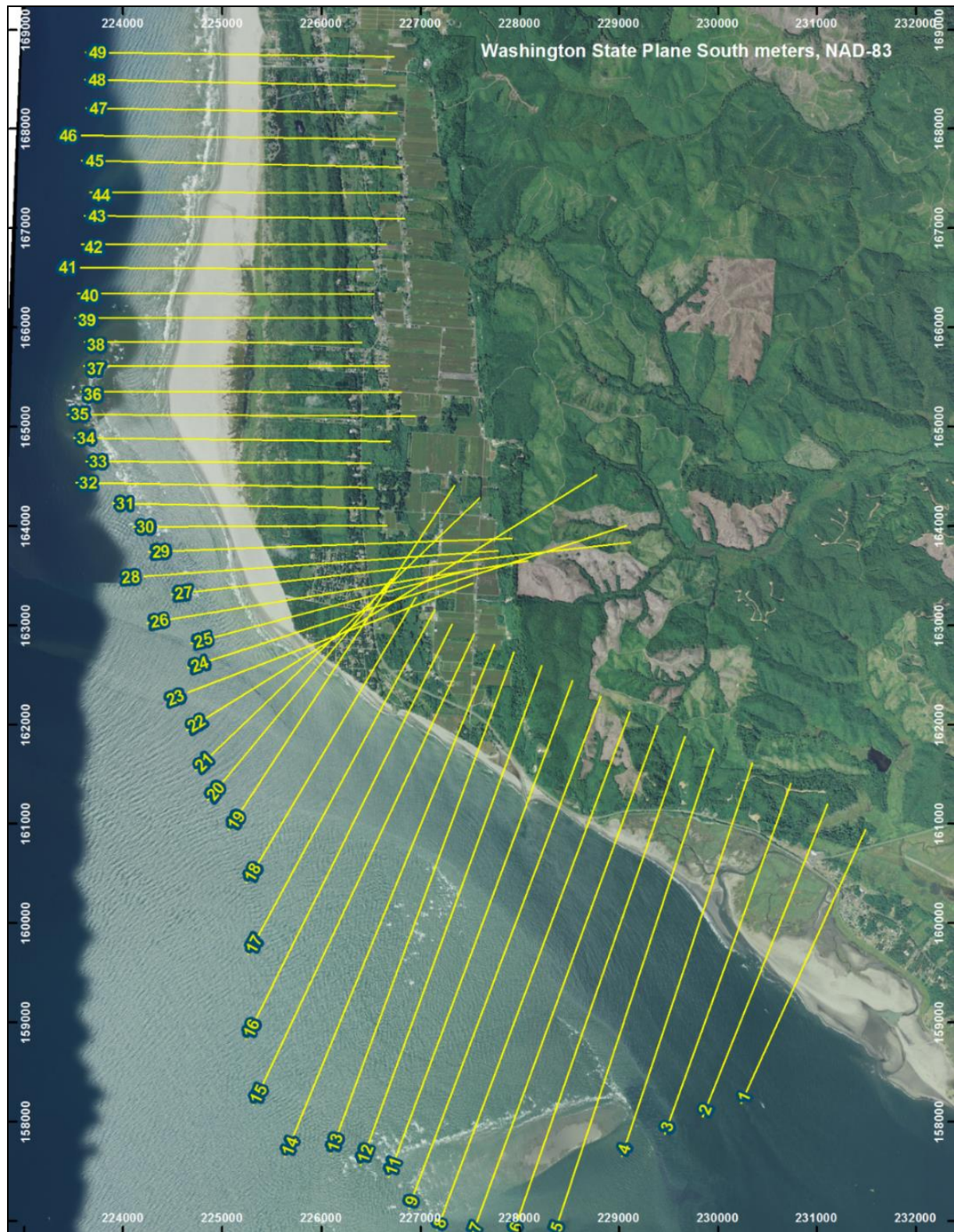


Figure 5: Map showing locations of cross-shore transects, drawn at roughly 200-meter intervals (± 100 meters) alongshore. The SR-105 groin is located at Transect 11 and the Pacific County line is just south of Transect 49.

At each of the 48 cross-shore transects, shoreline change vectors were calculated for every sequential interval of historical shorelines. For example, in Figure 6, the shoreline change vector at Transect 19 for the interval from 1974 to 1985 is 200, indicating that there was 200 meters of shoreline advance (accretion) between those two shorelines along that transect.

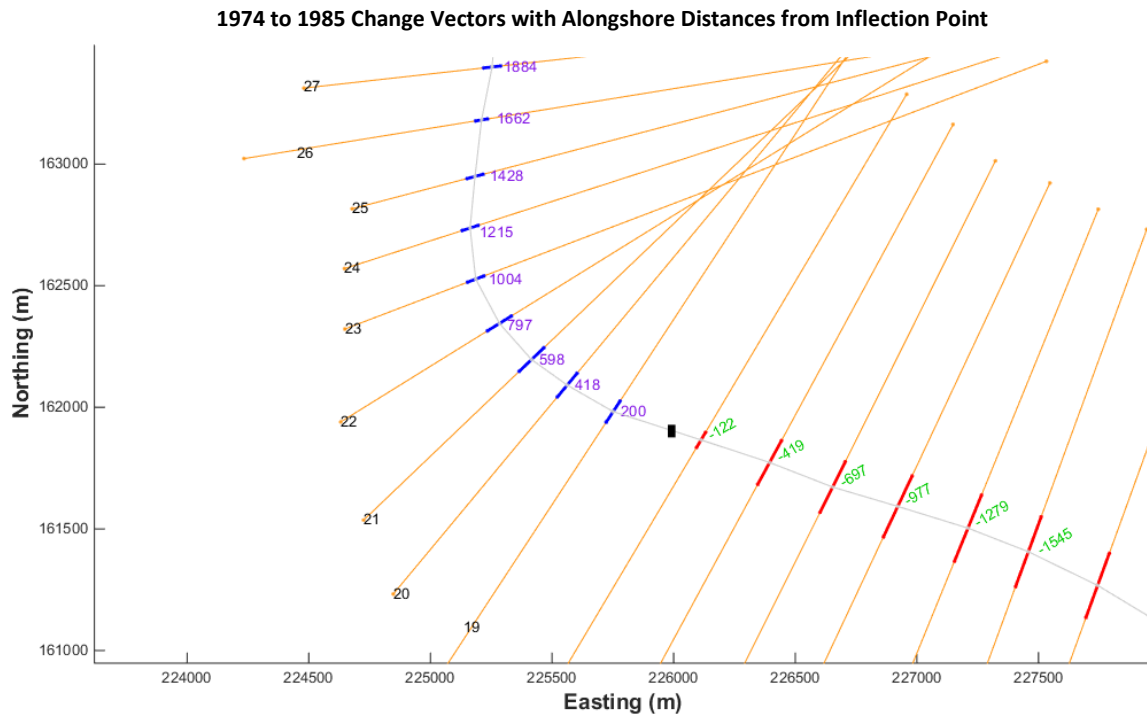


Figure 6: Shoreline change vectors for the interval between 1974 and 1985. The orange lines are the cross-shore transects as illustrated in Figure 5. Overlaid on them are blue and red line segments showing the change vectors between the 1974 and 1985 shorelines. Red indicates erosion (shoreline retreat) and blue indicates accretion (shoreline advance). The gray dotted line is the interval-average shoreline created by connecting the mid-points of each change vector. The numbers in green and purple indicate the alongshore distance of each change vector from its interval-relevant inflection point (shown as a black square, and discussed further in the text). The negative distances (in green) indicate an upstream direction (in terms of the Willapa Bay ebb current), and the positive distances (in purple) indicate the downstream direction.

Except for the 1911-1926 and 1963-1970 intervals, every sequential shoreline interval from the historical shorelines revealed a consistent switch (i.e., inflection point) between shoreline retreat along the Willapa Bay entrance toward the southeast and shoreline advance along the ocean coast toward the northwest. Figure 7 illustrates the inflection point between the 1871 and 1926 shorelines and shows the position of subsequent inflection points through time. For data-modeling purposes, each inflection point was assigned the average date between sequential shorelines.

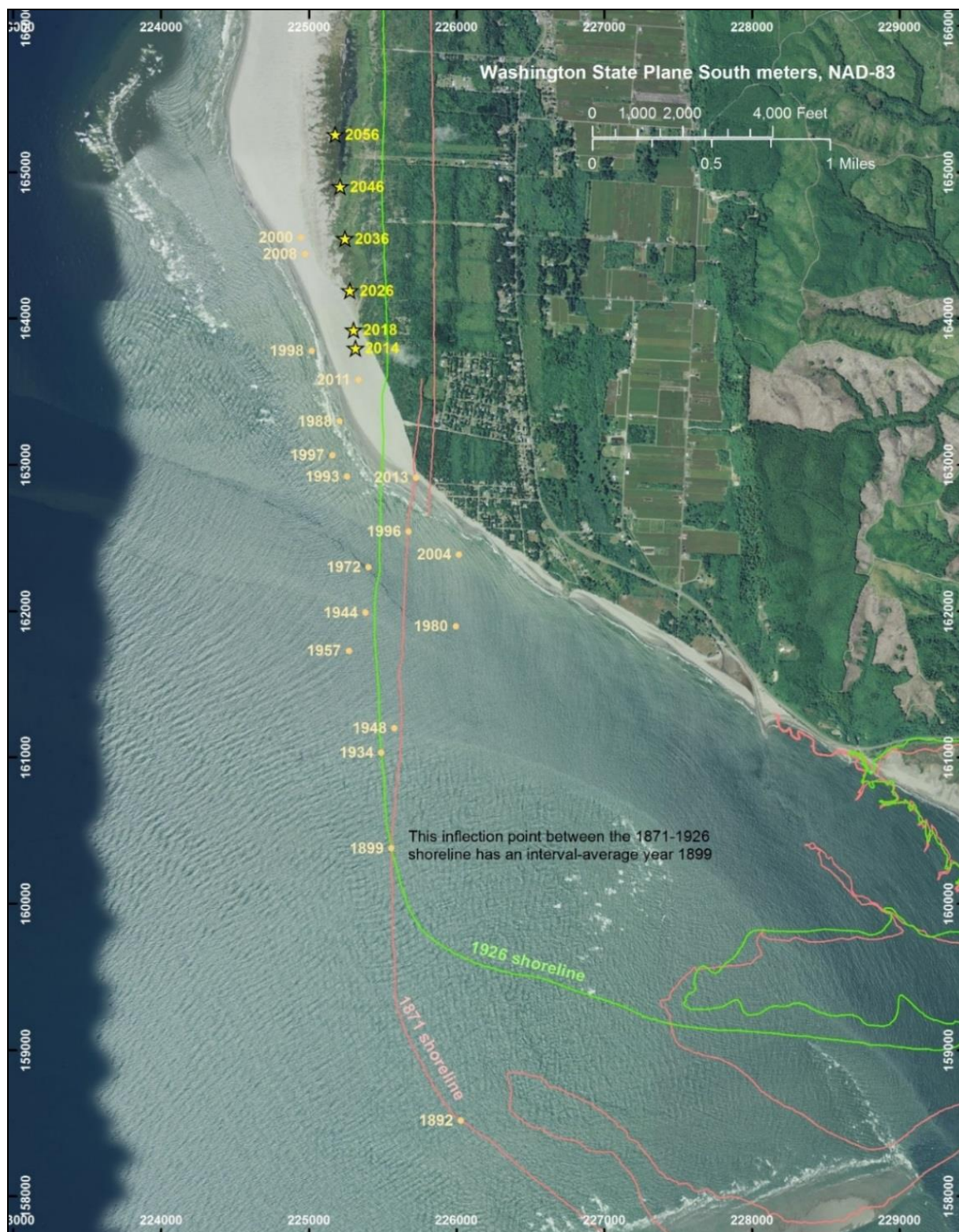


Figure 7: Map showing the 1871 and 1926 shorelines, depicting their inflection point between shoreline retreat in the southeast and shoreline advance in the northwest. This inflection point has an average date of 1899. Other historical shoreline inflection points and their interval-averaged dates are shown in yellow dots and text. Future modeled inflection points are shown in yellow stars.

Table 2 shows how the historical shorelines were applied in the change analysis. Some shorelines did not extend far enough northward to the Pacific County line to be included in the analysis. However, the shorelines could still be used to locate and model the inflection point for sequential time intervals.

Year of Shoreline	Used for Change Rate Analysis	Used for Inflection Point Analysis	Shoreline Pairings Used to Determine Inflection Points		
			FROM Year	TO Year	Interval-Average Year
1871.5	X	X	1871.5	1911.5	1891.5
1911.5	X	X	1871.5	1926.5	1899.0
1926.5	X	X	1926.5	1942.5	1934.5
1942.5	X	X	1942.5	1945.5	1944.0
1945.5		X	1945.5	1950.5	1948.0
1950.5	X	X	1950.5	1963.6	1957.0
1963.6	X	X	1970.5	1974.5	1972.5
1970.5		X	1974.5	1985.5	1980.0
1974.5	X	X	1985.5	1990.7	1988.1
1985.5	X	X	1990.7	1995.6	1993.2
1990.7		X	1995.6	1996.6	1996.1
1995.6	X	X	1996.6	1997.3	1996.9
1996.6		X	1997.3	1999.4	1998.3
1997.3		X	1999.4	2001.3	2000.4
1999.4	X	X	2001.3	2006.5	2003.9
2001.3		X	2006.5	2009.7	2008.1
2006.5	X	X	2009.7	2011.6	2010.7
2009.7	X	X	2011.6	2013.5	2012.6
2011.6	X	X			
2013.5	X	X			

Table 2: The 20 historical shorelines digitized and how they are utilized for analysis in this study.

Consistent with the findings of Kaminsky et al. (1999), the inflection points were observed to migrate northward, on average, at a rate of 35.6 meters per year (Figure 8).¹²

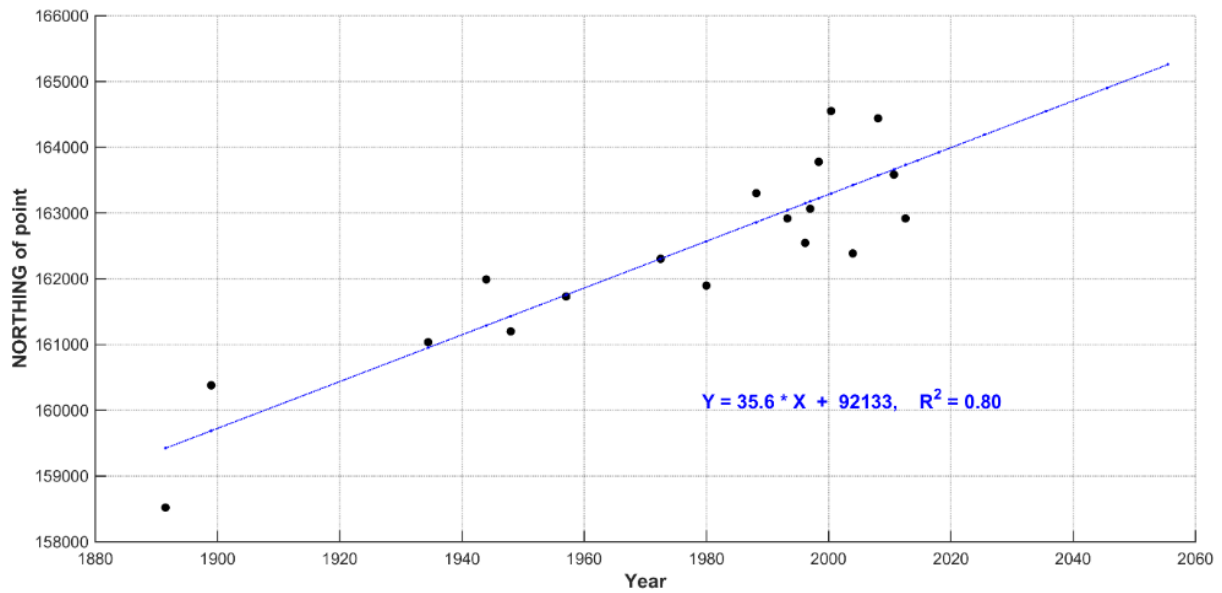


Figure 8: Data plot with the Northing coordinate of inflection points on the Y-axis versus year on the X-axis, showing a strong trend ($R^2 = 0.8$) of linear northward migration. The slope of the line, $Y = 35.6 * X$ indicates that the Northing coordinate of the inflection point increases by 35.6 meters per year.

Figure 9 shows historical shoreline change rates for each transect, numbered from 1 to 49 from southeast to northwest.

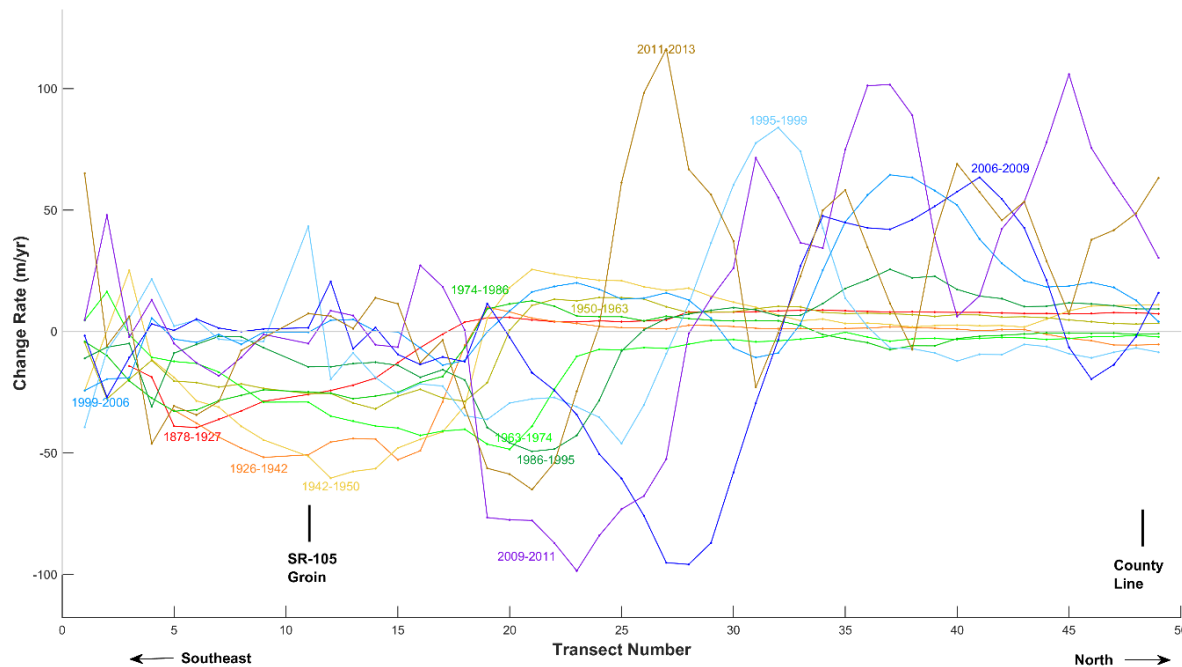


Figure 9: Historical shoreline change rates plotted as a function of the transect number.

In order to project future shoreline positions, both historical shoreline change data and the northward migration of the inflection point needed to be integrated into a common reference frame which moves through time. As illustrated in Figure 10, each shoreline change vector was assigned an alongshore distance away from its interval-averaged inflection point. Change vectors were then analyzed by their position in a moving reference frame (i.e., their distance along the shoreline from the northward-migrating inflection point) rather than in absolute geographic space. An average shoreline change rate was calculated from the historical change rates at 100-meter intervals from their associated inflection points (Figure 10). The average of all shoreline change vectors is shown in a heavy black line and shows consistent shoreline behavior with negative change rates (shoreline retreat; erosion) occurring upstream (south) of the inflection point and positive change rates (shoreline advance; accretion) occurring downstream (north) of the inflection point. The shoreline change rates for 1999-2006 and 1963-1974 have modeled inflection points, thus they are slightly offset.

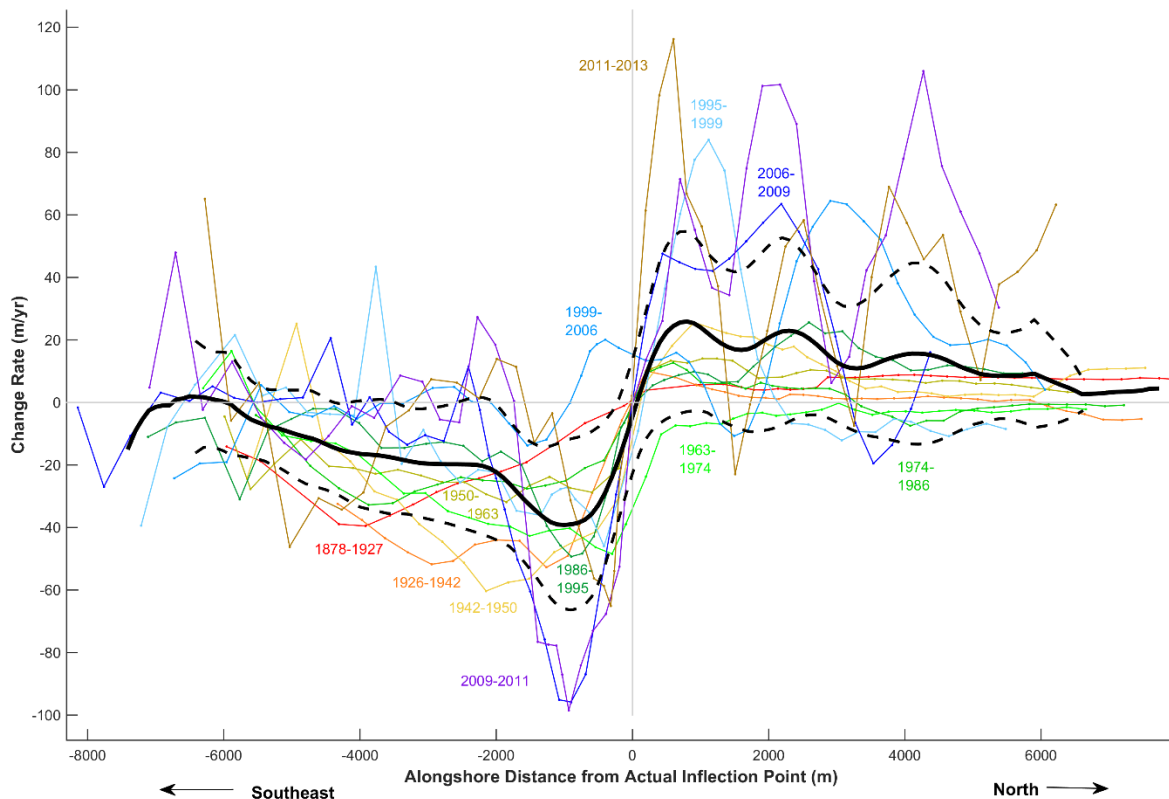


Figure 10: Historical change rates relative to alongshore distance from the associated interval-averaged inflection point. The black line shows the average shoreline change rate as a function of alongshore distance from the inflection point, and the dashed black lines represent one standard deviation away from the average shoreline change rate. The alongshore distance is measured cumulatively along the orientation of the shoreline at each transect.

Predicted future shorelines for the years 2015, 2020, 2030, 2040, 2050, and 2060 were created using the average shoreline change rate transposed onto a moving reference frame (the migrating inflection point). The predictions start with the earliest shoreline (2015) and work forward in time, as each predicted shoreline represents the seed for the next prediction. For each subsequent year, the modeled position of the inflection point (migrating northward at 35.6 meters per year) was projected onto the earlier of the two shorelines to determine the reference frame origin for that predicted shoreline. Transects were then segregated into upstream and downstream portions relative to the modeled future inflection point. The shoreline change rate for each transect was then projected off of the prior shoreline to determine the future shoreline position. Shoreline change statistics including the mean and standard deviation were calculated so that the uncertainty of the predictions could also be mapped.

Extreme Water Levels

CMAP worked closely with Oregon State University (OSU) to improve the robustness of the erosion predictions by assessing hazards associated with extreme water levels. OSU examined the effects of elevated water levels that directly cause erosion, flooding, and dune overtopping and took into account the elevation and volume of the uplands. Previous studies have demonstrated that erosion and flooding potential is correlated with the total water levels (TWLs) that result from a combination of astronomical tides, atmospheric pressure anomalies, wind stress, ocean waves breaking on the Willapa ebb shoals and wave run-up at the toe of the uplands.

Extreme coastal TWLs are the result of interactions between multiple oceanographic, hydrological, geological and meteorological forcing's that act over a wide range of scales (e.g., astronomical tide, wave setup, large-scale storm surge, monthly mean sea level, vertical land motions (VLM), etc.). At any given time, the elevation of the TWL, relative to a fixed datum, is comprised of two components such that

$$TWL = SWL + R \quad \text{Eq. 1}$$

Where the *SWL* is the still water level, or the measured water level from tide gauges, and *R* is a wave induced component, termed the wave runup. The wave runup calculation is often dependent on the wave height, wave length, and the local beach morphology (e.g., Holman and Sallenger, 1986; Ruggiero et al., 2001, Stockdon et al., 2006), making it a highly site-specific computation.^{13,14,15} Because we are interested here primarily in extreme events, *R* is parameterized using *R*_{2%}, corresponding to the 2% exceedance percentile of runup maxima.

The *SWL* can further be broken down into

$$SWL = MSL + \eta_A + \eta_{NTR} \quad \text{Eq. 2}$$

Where *MSL* is the mean sea level, η_A is the deterministic astronomical tide, and η_{NTR} is the non-tidal residual, or any elevation change to the water level not due to the tide. The elevation of the η_{NTR} is often driven by changes in the seasons, storm surges produced by discrete storm events, and interannual variability due to the El Niño Southern Oscillation (ENSO), a periodic change in the large-scale climate caused by variations in sea surface temperatures over the tropical eastern Pacific Ocean. The warming phase is termed El Niño, while the cooling phase is known as La Niña. During El Niño years, the PNW coastline experiences increased water levels for months at a time, along with changes in the frequency and intensity of storm systems (Komar 1986; Allan and Komar, 2002).^{16,17} From Equations 1 and 2, TWL time series can be constructed based on observational records of waves and water levels (e.g., Ruggiero et al., 2001).¹⁸

OSU undertook the following steps while assessing extreme water levels:

1. Develop a combined wave and water level time series from measured and hindcast data relevant to study area
2. Extract backshore morphology and beach slope from LIDAR data

3. Develop TWL time series using a 'structural function' approach (Ruggiero et al. 2001).¹⁹
4. Compare various TWL statistics to the backshore morphology using Sallenger's (2000) Storm Impact Scale.²⁰
5. Compute extreme TWL return levels using the Peak Over Threshold method
6. Assess the relative exposure of Washaway Beach

In step 1, a 35-year combined wave and water level time series was developed using the following data:

Waves - Combined Grays Harbor Buoy (CDIP 0036/NDBC 46211) with WIS 83011 (closest WIS station to this buoy)

Water levels - Used measured water levels from the Toke Point Tide Gauge (NOAA station #9440910)

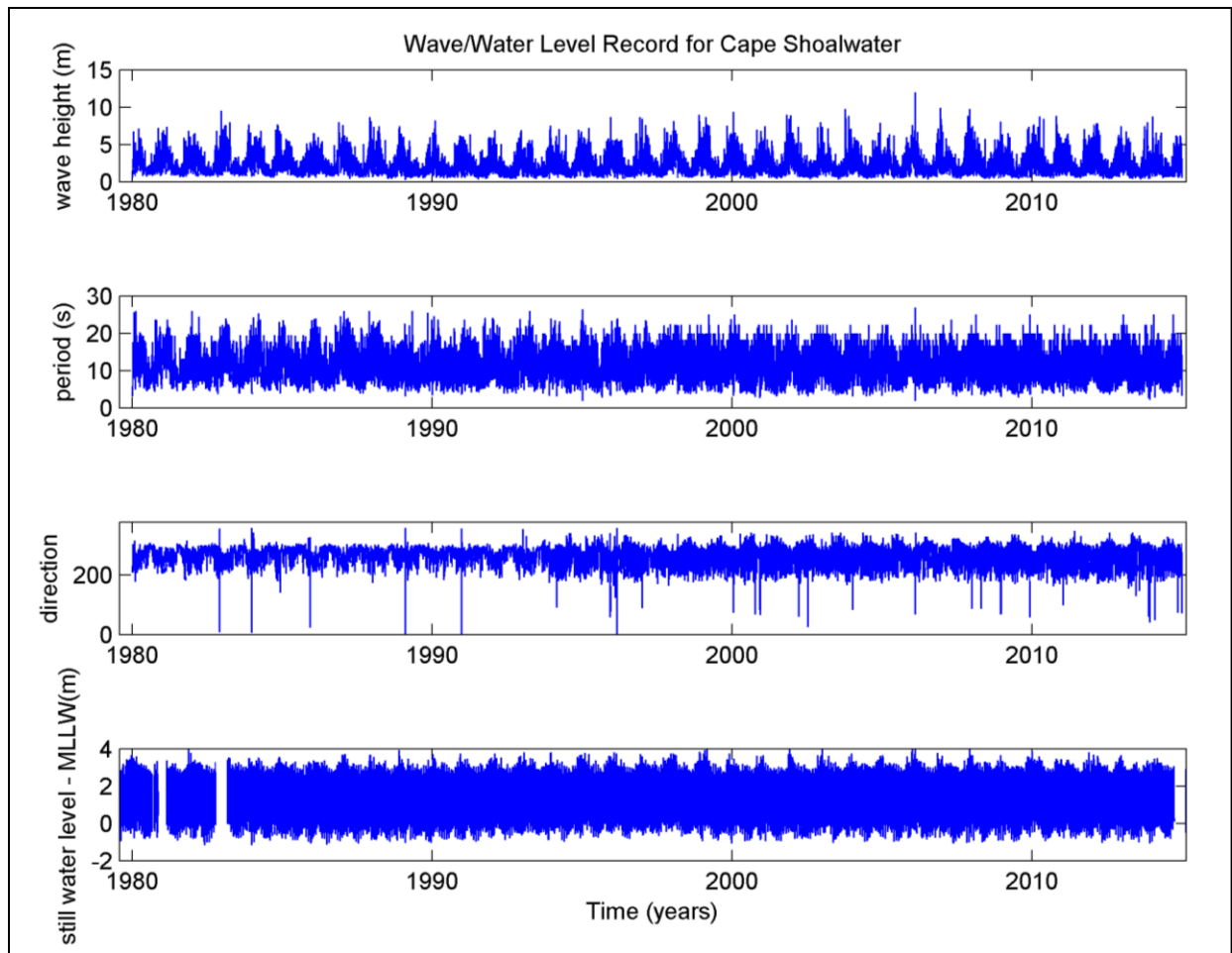


Figure 11: Combined wave and water level time series for assessing extreme TWLs at Washaway Beach.

In step 2, beach morphology (dune crest (z_c), dune toe (z_t), and beach slope) was extracted from a 2010 Lidar survey of the region using the methods developed by Mull and Ruggiero (2014).²¹

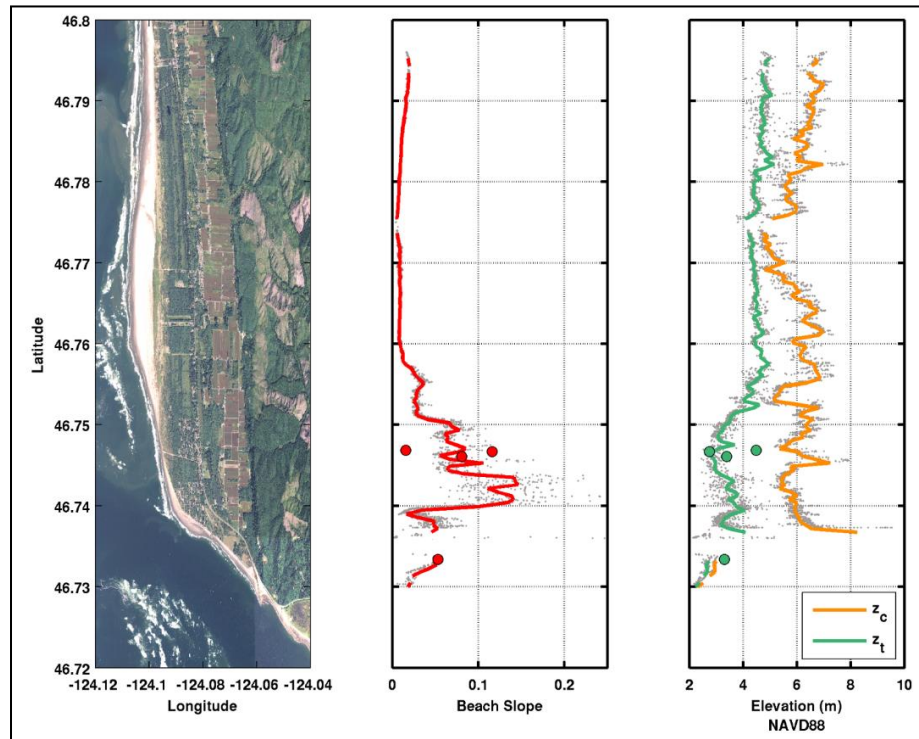


Figure 12: Beach morphometrics at Washaway Beach.

In step 3, we combine two different approaches for computing TWLs along Washaway Beach as outlined in Figure 14.

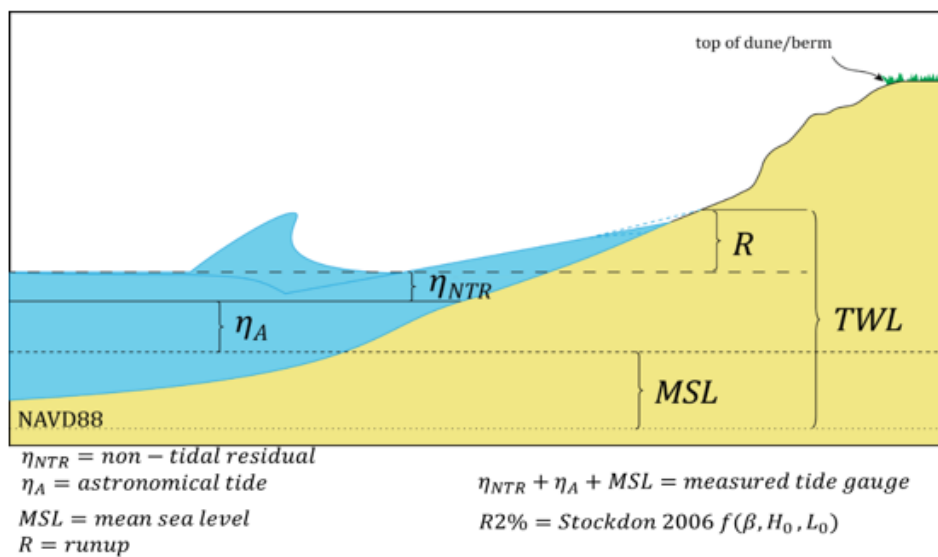


Figure 13: Applying the TWL modeling approach of Ruggiero et al. (2001) and Serafin and Ruggiero (2014).^{22, 23}

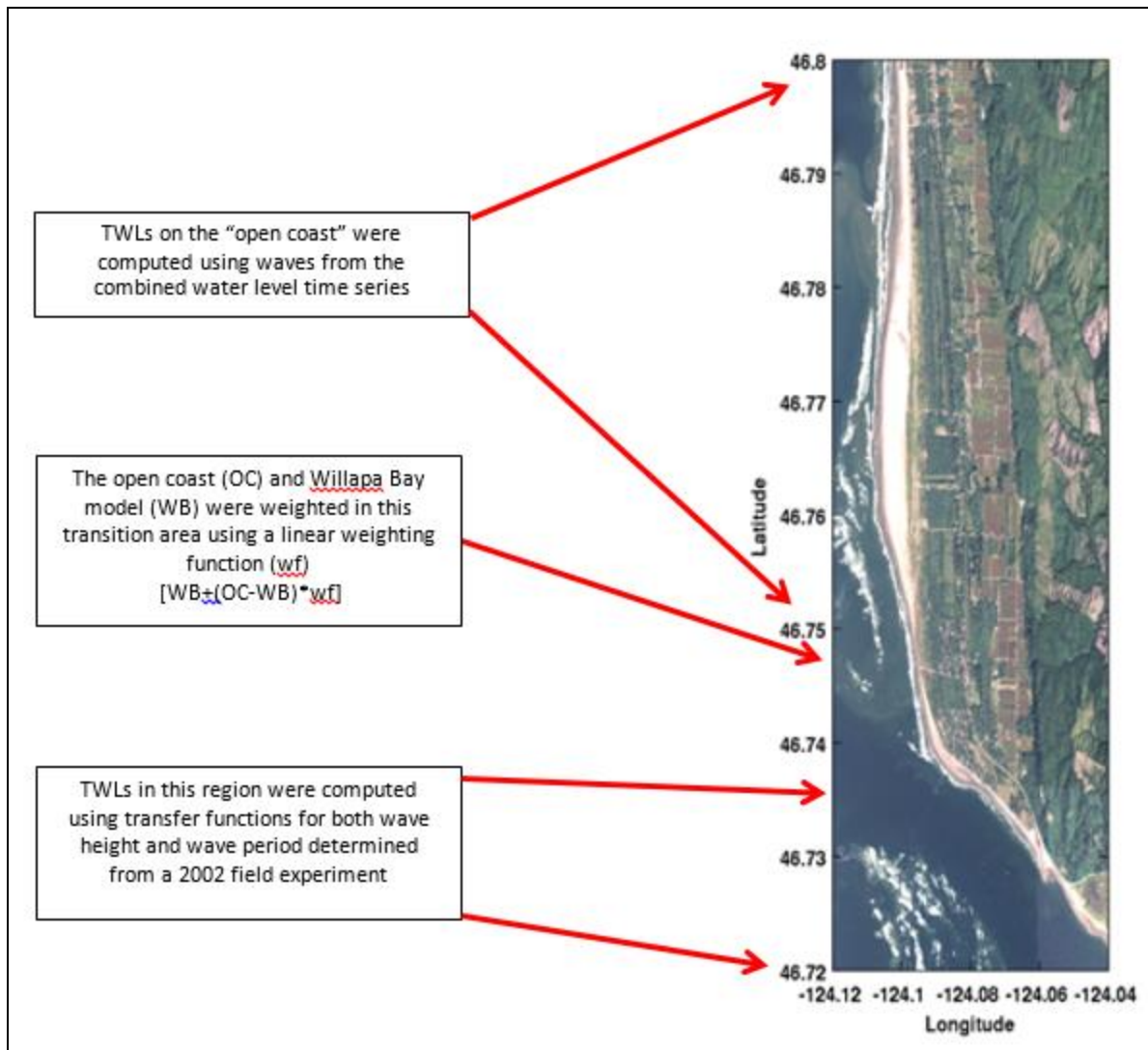


Figure 14: Explanation of use of 'Open Coast' vs 'Willapa Bay' Models. The 'Open Coast' approach for computing TWLs follows Equations 1 and 2 above and simply uses the combined wave and tide time series. The 'Willapa Bay Model' was developed due to the fact that waves dissipate energy along the ebb-tidal delta of Willapa Bay so using conditions measured offshore is not appropriate. Here we use results from a 2002 field experiment led by the USGS in which a simple transfer function between observed water level at Toke Point, and wave height of the channel was developed. While certainly a significant simplification, this approach allows us to make more reliable estimates of TWLs along the protected stretches of Washaway Beach without the expense of a sophisticated numerical model. In the area between the two regions a simple linear smoothing function is used to give smoothed results between the two domains.

By comparing the elevations achieved by TWLs to the extracted coastal morphology metrics (Figures 12, 13, and 14), we can effectively determine the risk to overtopping and erosion for a section of coastline (Sallenger, 2000; Ruggiero et al., 2001; Stockdon et al., 2007, Ruggiero, 2013).^{24, 25, 26, 27} In the Storm Impact Scaling model, four storm-impact regimes, or thresholds for coastal change, are defined to provide a framework for examining the relative magnitudes of coastal change likely to occur (Sallenger, 2000).²⁸ Here we only apply two of the regimes,

collision ($z_t \leq \text{TWL} < z_c$) and overtopping ($\text{TWL} \geq z_c$; Figure 16). Each of these regimes has implications for varying levels of morphologic change. In the collision regime, the water level is impacting the backshore feature, resulting in its erosion or possible damage to engineered structures. In the overtopping regime, the water level is over the z_c and the possibility exists for inundation of the backshore (Sallenger, 2000; Figure 15).²⁹

In this application, the Storm Impact Scale is used to estimate how exposed a coastline is to nuisance hazards, and collision and overtopping “days per year” are calculated (IDPY; ODPY). This provides an average amount of time the coastline experiences one of the two regimes (during the highest water level of the day), thus an estimate of a particular stretch of coastline’s exposure to everyday hazards. Extreme events, such as the annual maximum event or the 100-year return level (i.e., a 1% chance of occurrence annually) can also be compared to the extracted morphology to assess the exposure of a particular study area to a specified extreme event scenario.

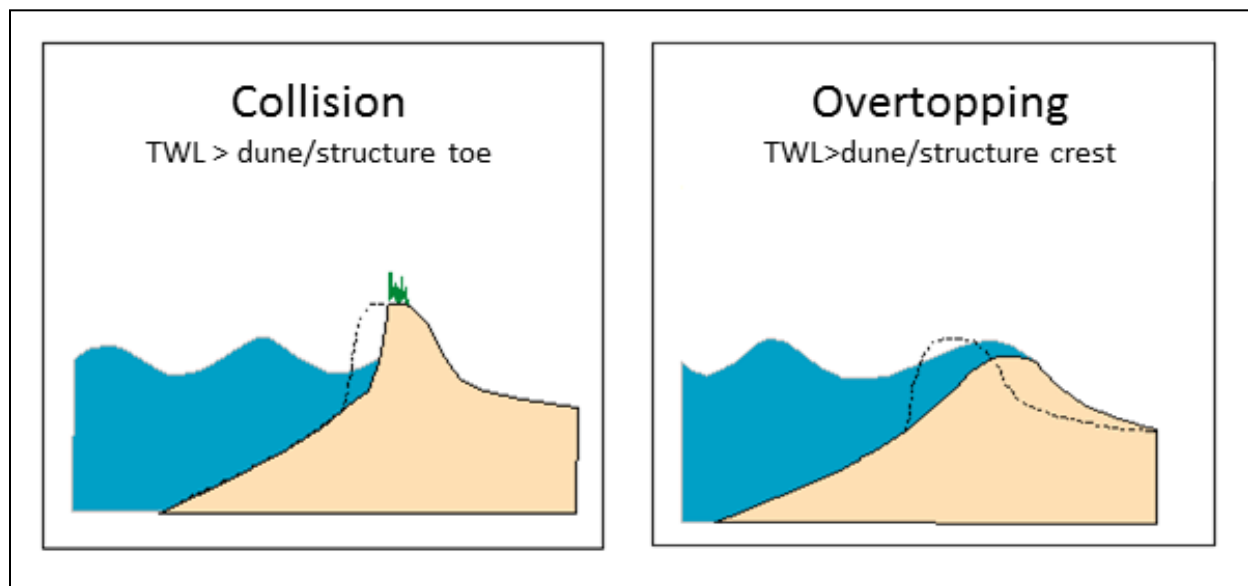


Figure 15: Schematics representing the two Storm Impact regimes of interest in this study (modified from Sallenger 2000), collision or overtopping. Collision is when the $\text{TWL} > z_t$ and overtopping occurs when the $\text{TWL} > z_c$.

This assessment was critical to the project because it included robust projections of the future shoreline position defining land area likely to be lost over increments at a scale that meets the immediate and long-term management needs of the North Cove community. It also serves as an important and successful application and use of existing data that is currently available to all communities along Washington’s outer coast.

Erosion Assessment

The projections of future shoreline change are essential for long-term planning and the identification of areas having the highest vulnerability to erosion and flooding are important for guiding near-term efforts.

The projected future shorelines are shown in Figure 16. These same projected shorelines are shown in terms of shoreline change rates in Figure 17. These figures show the anticipated erosion along the southwest-facing entrance to Willapa Bay associated with the northern migration of the entrance channel and further driven by wave forcing and elevated water levels. The projected shorelines also show the continued accretion of the westward-facing shoreline associated with the northward migration of the shore-attached ebb shoal. It is important to note that the shoreline approximates the average high-water line during summer, which is located along the upper beach and relatively close to the erosion scarp and vegetation line along the southwest-facing shoreline, and relatively far from the vegetation line along the westward-facing shoreline as illustrated by the 2015 predicted shoreline plotted on the 2013 aerial photo image. The beach along the westward-facing shoreline is relatively wide and flat because of its attachment to the broad ebb shoal offshore. The ebb shoal is apparent in Figure 20, which shows the 2015 predicted shoreline on a 2015 aerial photo image along with the uncertainty in shoreline position based on \pm one standard deviation from the mean shoreline, which statistically represents a 63% chance the shoreline will be within those bounds.

Appendix B shows the 2020, 2030, 2040, 2050, and 2060 predicted shorelines, plotted on the 2013 aerial photo imagery along with the uncertainty in shoreline position expressed by \pm one standard deviation from the mean shoreline. Note that the uncertainty increases with time into the future since each subsequent predicted shoreline is dependent on the starting position of the previously predicted shoreline. The most landward shoreline uncertainty occurs if the actual shoreline change rates are always at the high end of the one standard deviation range, whereas the most seaward shoreline occurs if the actual shoreline change rates are always at the low end of the one standard deviation range. While the uncertainty shown is statistically sound, there is little physical basis or historical trend to expect that shoreline change along the southwest-facing shoreline would always occur at the low end of one standard deviation, because this would effectively involve a halting of the northerly migration of the entrance channel, which is not expected to occur within the next several decades. On the other hand, large episodic erosion events in the past have substantially exceeded annual average rates of erosion, thus there is a physical basis to anticipate that the erosion magnitude and resulting future shoreline position may be at least temporarily more landward than suggested by the mean shoreline location.

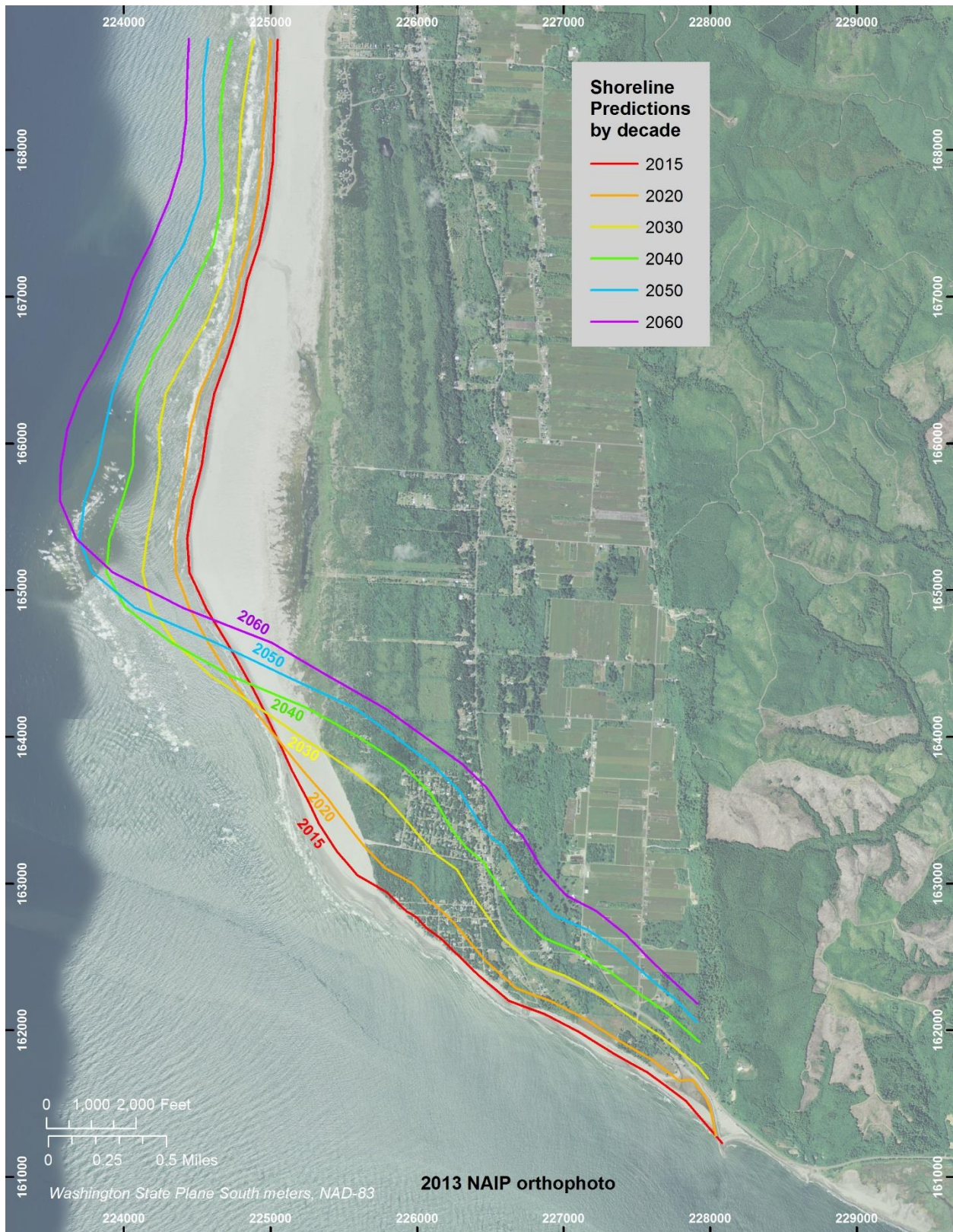


Figure 16: Map showing the predicted shorelines resulting from the Transposed Reference Frame technique described in the methods section.

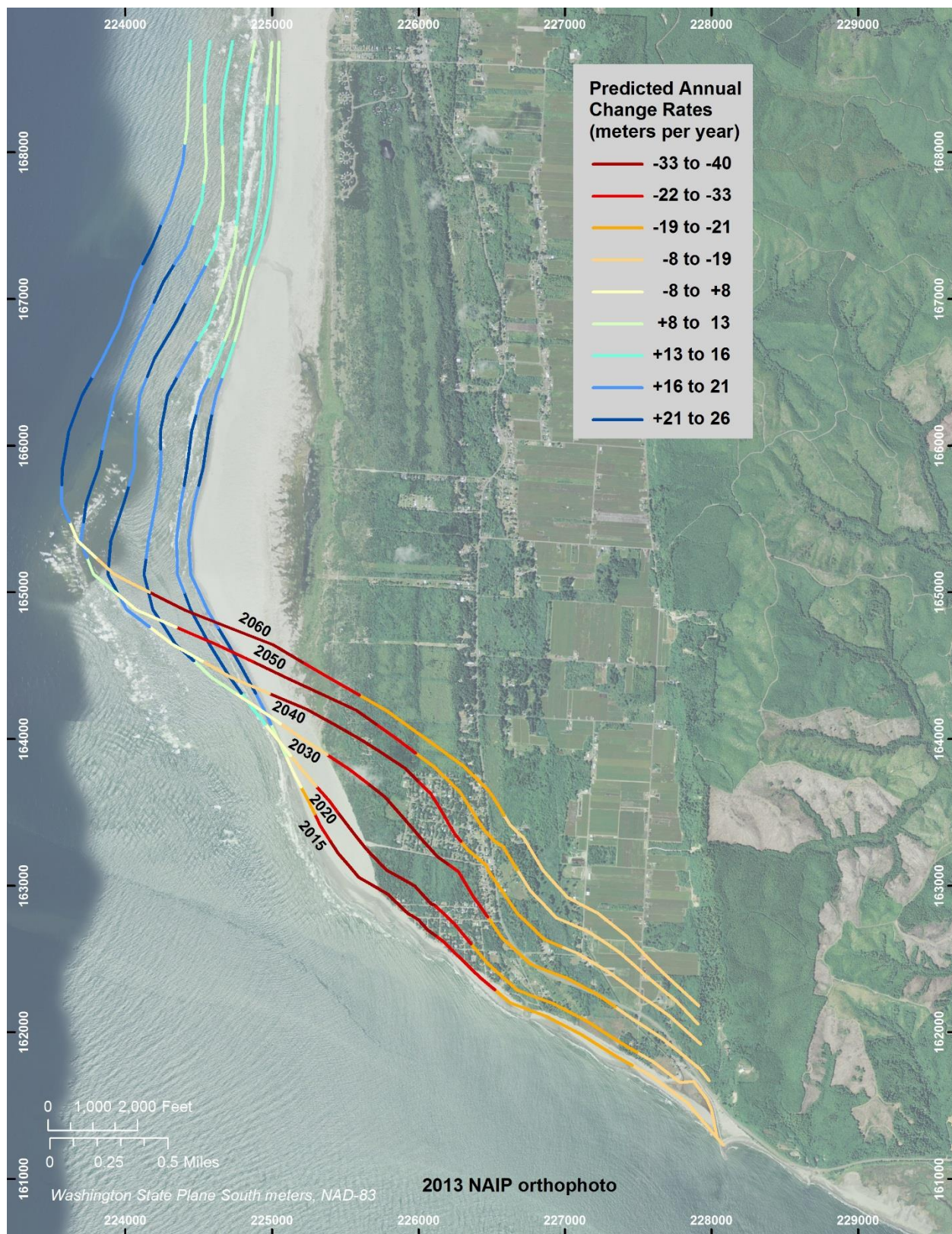


Figure 17: Map showing the predicted shorelines expressed in terms of shoreline change rates.

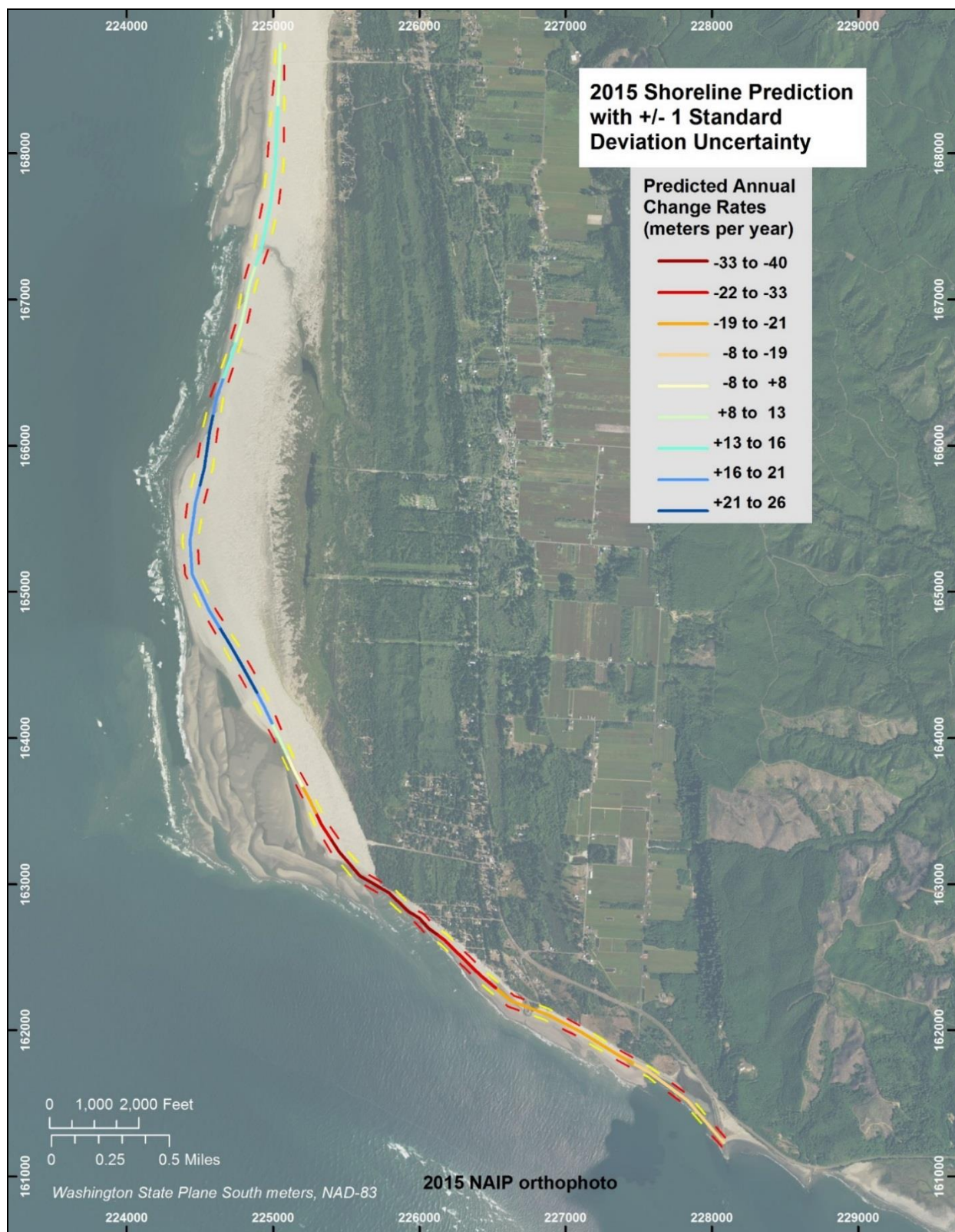


Figure 18: Map showing the predicted 2015 shoreline expressed in terms of shoreline change rates along with uncertainty in position based on +/- one standard deviation (dashed yellow and red lines). The 2015 predicted shoreline agrees reasonably well to the actual shoreline change between 2013 and 2015.

The results of modeling the effect of extreme water levels along the shoreline are presented in Figures 19-23. This modeling was conducted in an attempt to verify the findings from the historic shoreline change modeling. This modeling overwhelmingly aligns with and corroborates the findings based on historic shoreline change modeling listed above.

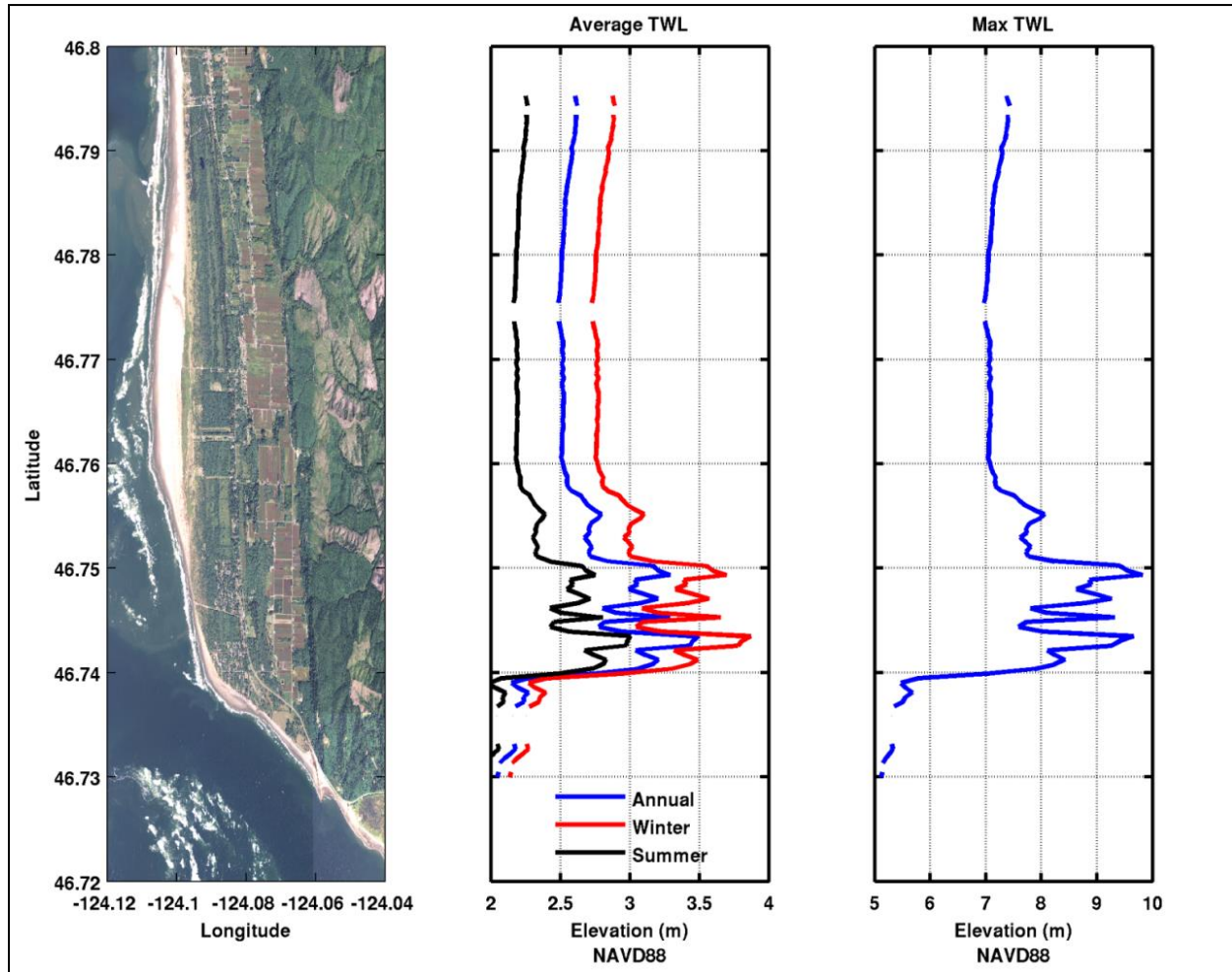


Figure 19: The alongshore variability of the annual average (blue), winter average (red) and summer average (black) TWLs along Washaway Beach. Note the ~1.0 m difference between summer and winter conditions. The right panel is the maximum TWL achieved during the historical time period (1980-2015) as computed using the combined time series.

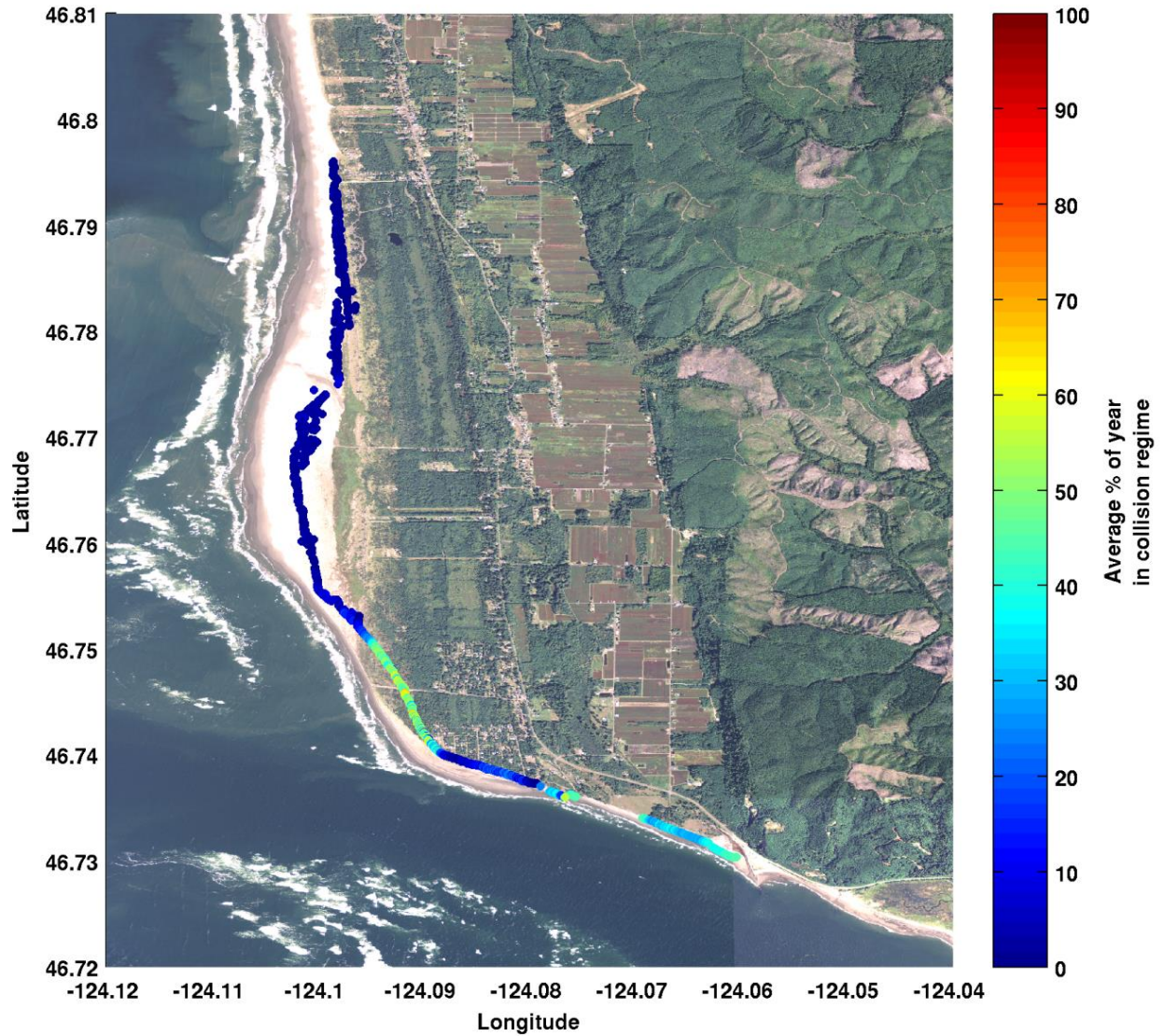


Figure 20: Map showing model results using the TWL time series and the Sallenger (2000) Storm Impact Scaling model, to predict how often certain stretches of coast are in the collision regime.³⁰ The analysis suggests that the most rapidly eroding section of Washaway Beach is indeed in the collision regime a high proportion of the time (>50%). This analysis is completely independent of the shoreline change analysis presented above and gives an indication of the processes responsible for the shoreline retreat along the westward-facing shoreline that adds to the erosion caused by the northerly migration of the entrance channel along the southwest-facing shoreline.

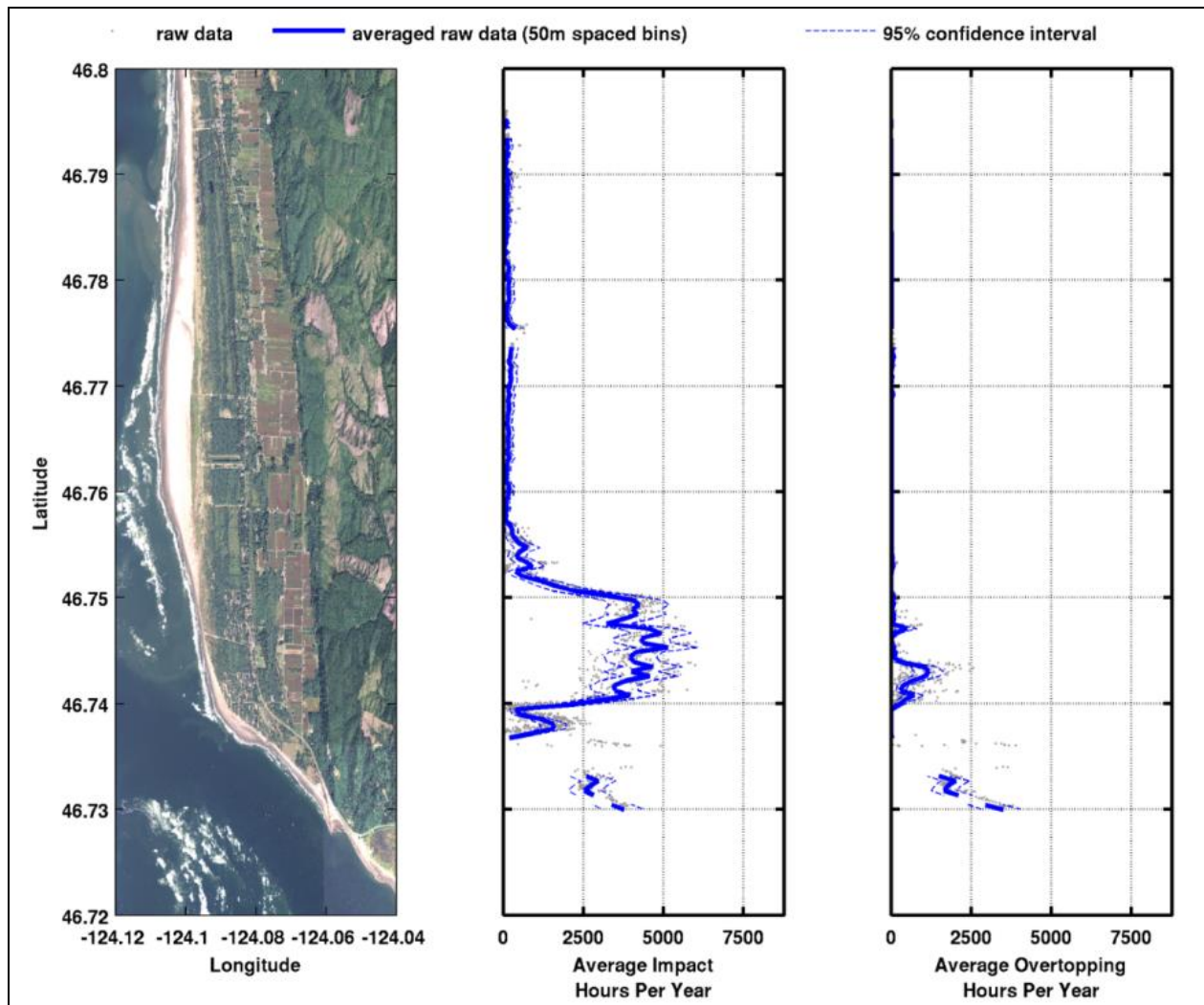


Figure 21: Summary of the annual average number of impact hours and overtopping hours per year. Areas with low crest elevations are predicted to be overtopped frequently.

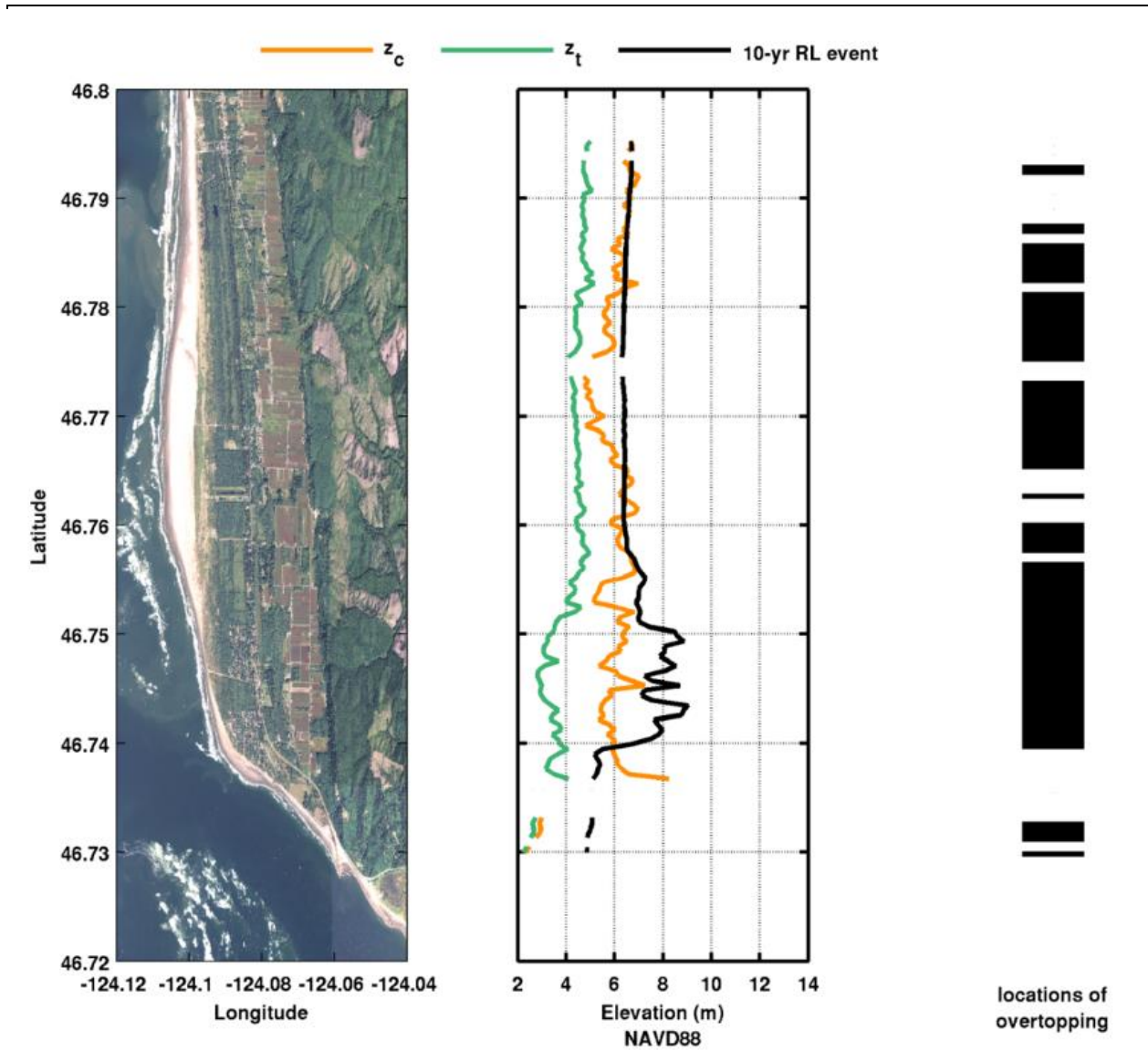


Figure 22: Elevation of TWLs for the 10-year return level event relative to backshore morphology. The black bars on the right indicate areas overtopped for this extreme event (75% of this stretch of coast). Note that z_c is low in some locations north of 46.76N due to the rapidly prograding coast in this area. Clearly the prediction of overtopping does not imply catastrophic flooding in these locations.

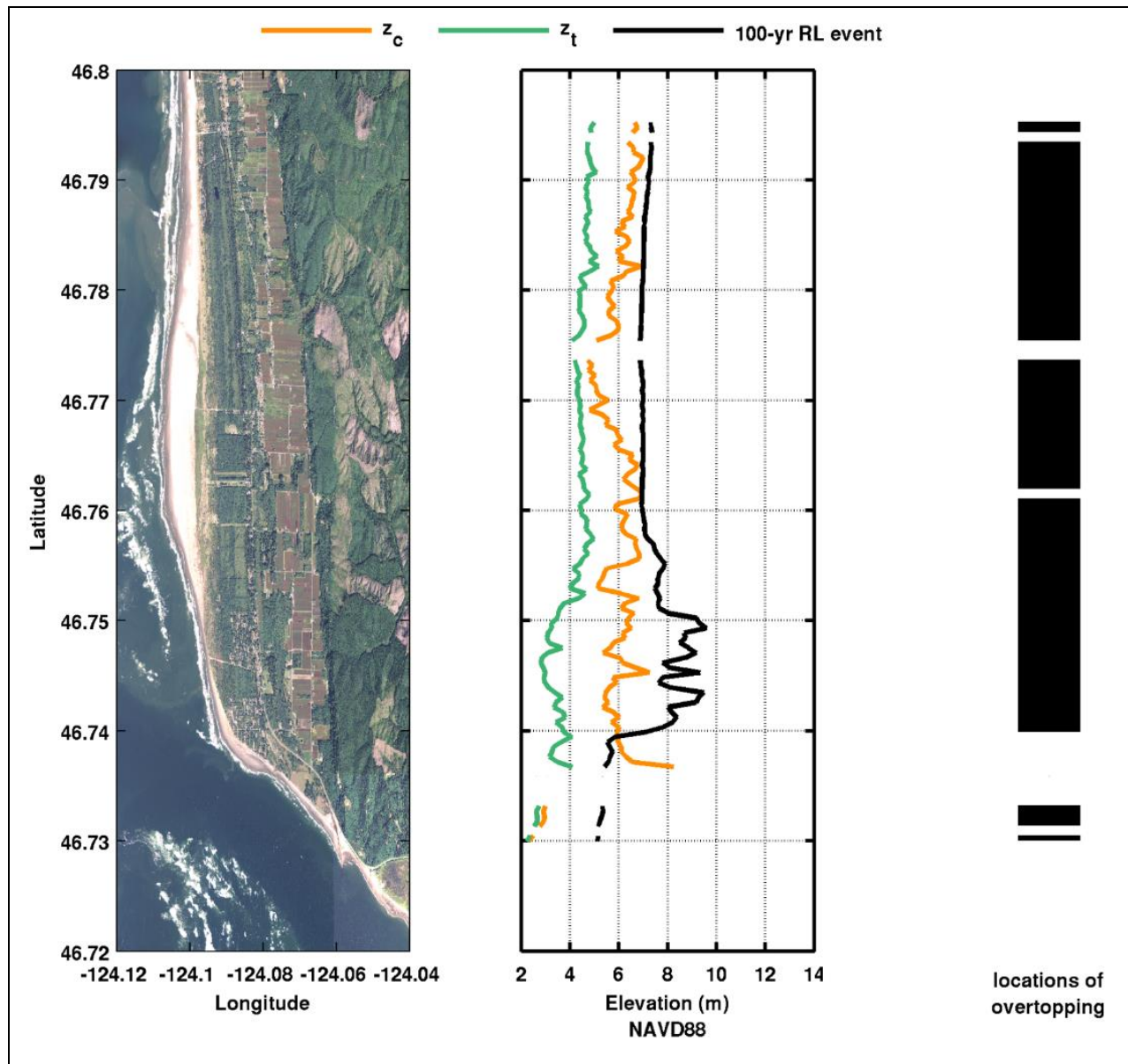


Figure 23: Elevation of TWLs for the 100-year return level event relative to backshore morphology. The black bars on the right indicate areas overtopped for this extreme event (87% of this stretch of coast). Note that z_c is low in some locations north of 46.76N due to the rapidly prograding coast in this area. Clearly the prediction of overtopping does not imply catastrophic flooding in these locations.

It is evident that both the future projections of shoreline change and the assessment of extreme water levels affecting coastal erosion independently find that the area of highest impact at present and over the long-term centers on an area in the vicinity of the Warrenton Cannery Road. Figure 24 combines the results of both methods (Figures 16 and 20) to illustrate the common area having the highest vulnerability to erosion (and flooding).

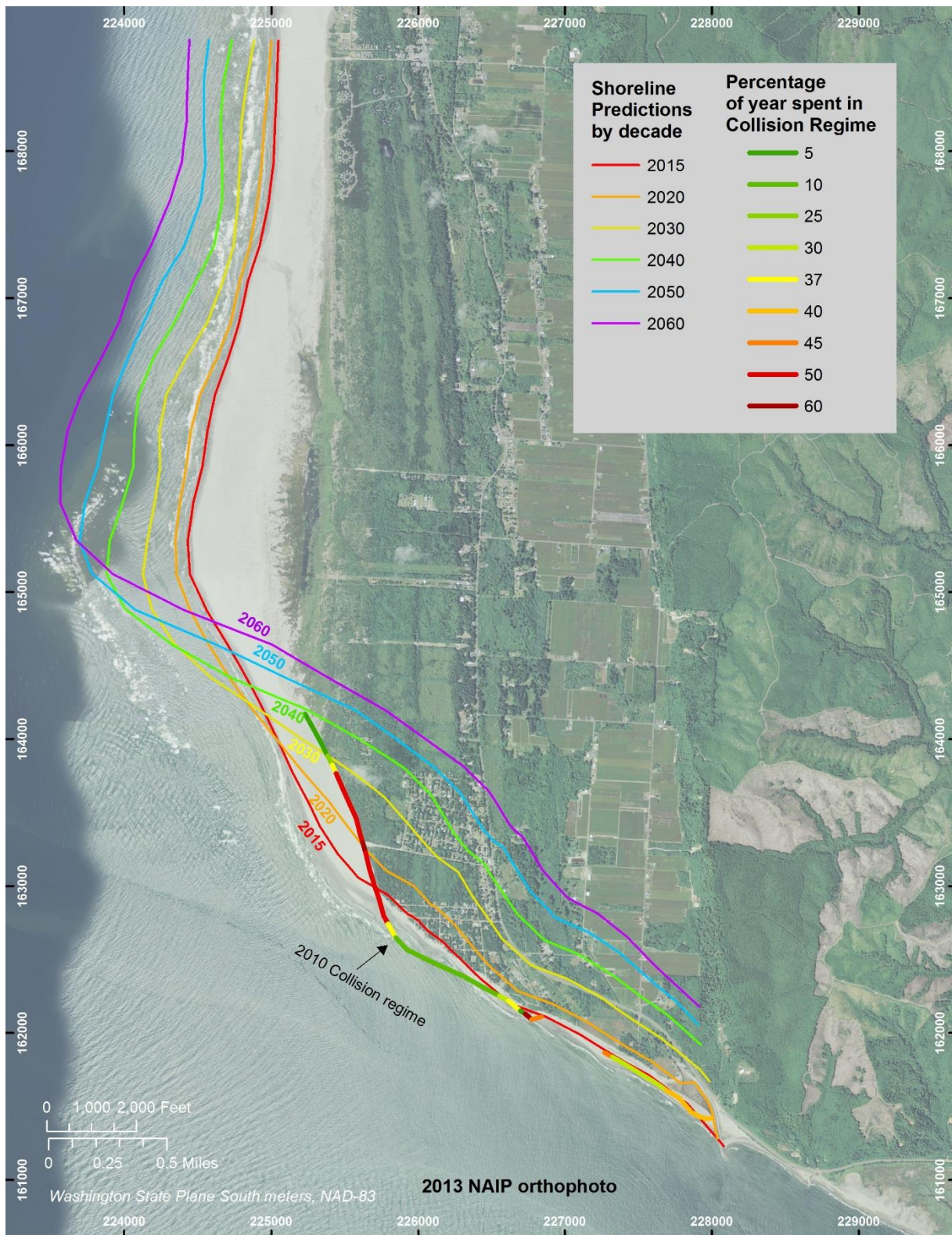
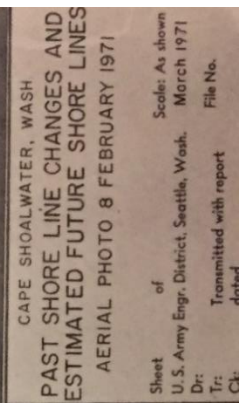
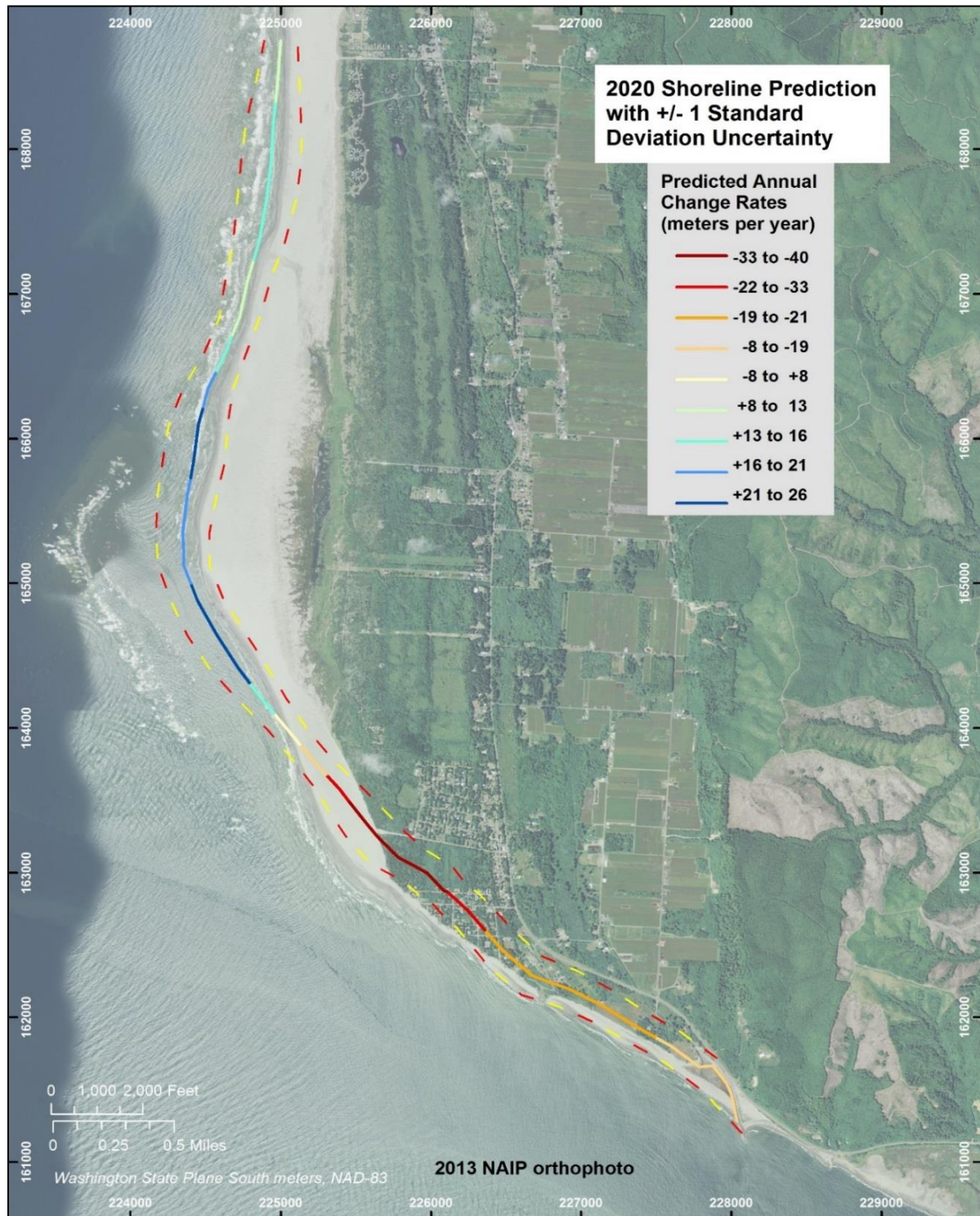


Figure 24: Map showing the predicted shorelines and the TWL model results for the collision regime. These results reveal that independent analyses both converge on the area in the vicinity of the Warrenton Cannery Road, the area most vulnerable to erosion (and flooding) aside from the southwest-facing shoreline, which is impacted by the northerly migration of the entrance channel.

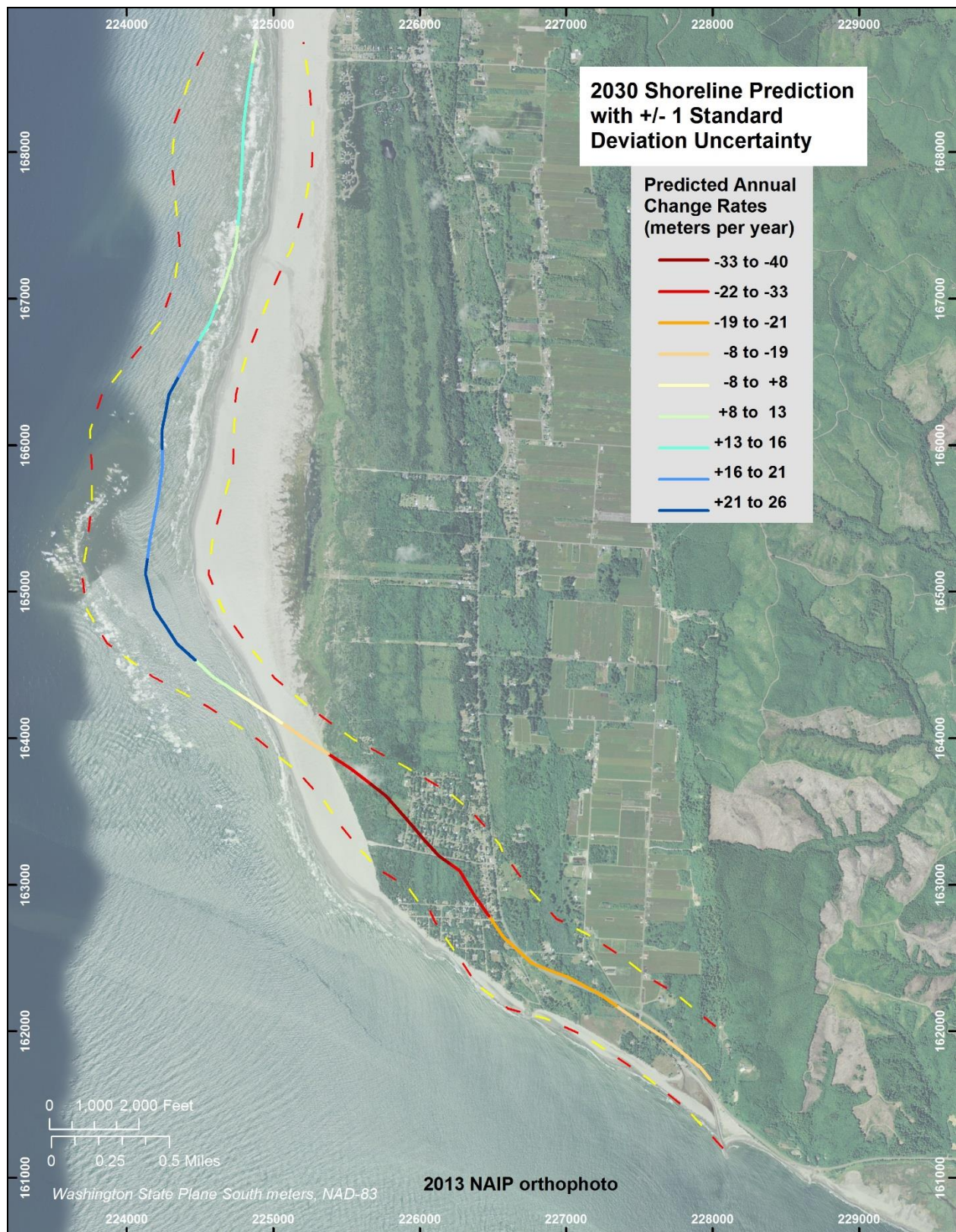
Appendix A – Past Shoreline Changes and Estimated Future Shorelines (1971)



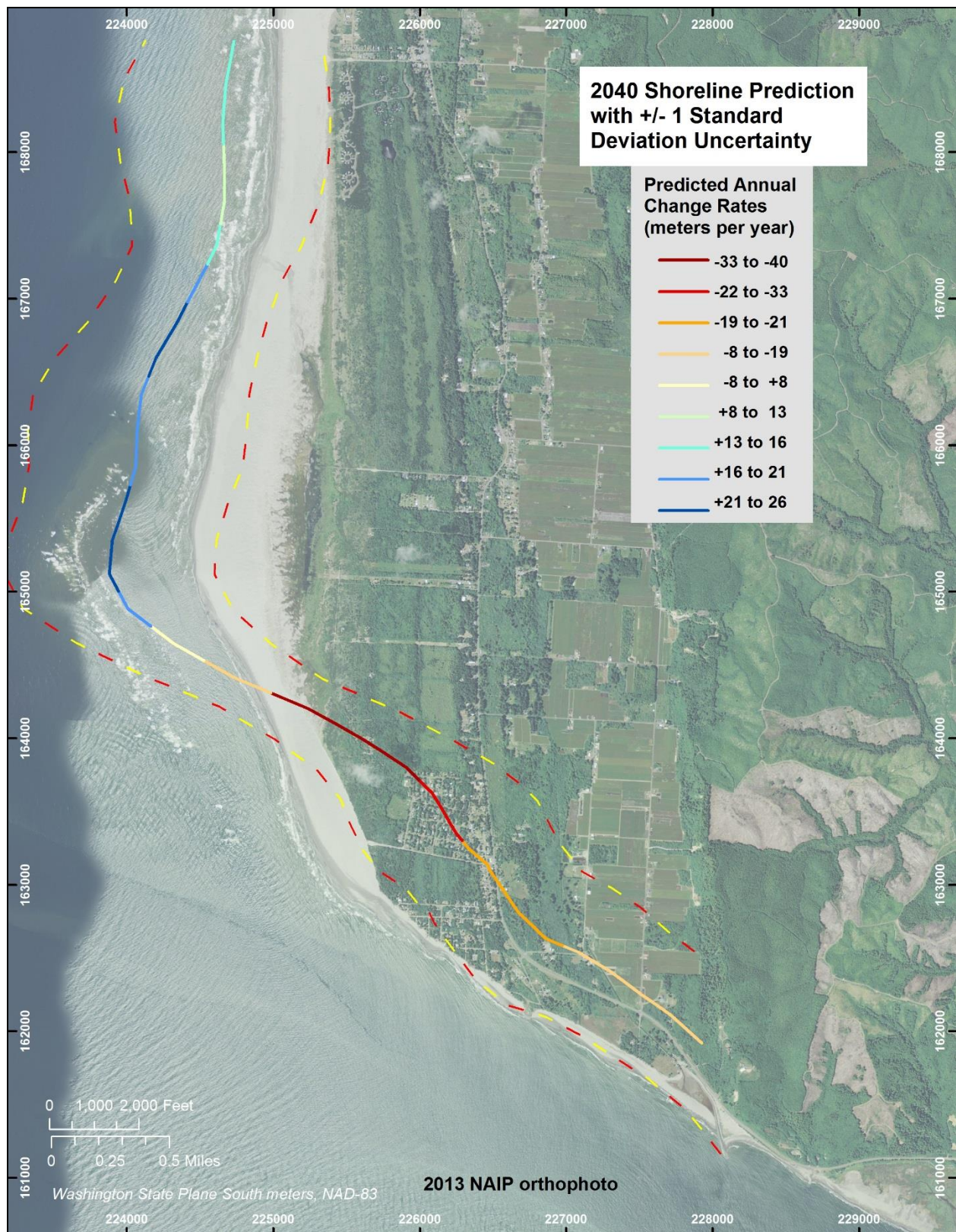
Appendix B – Shoreline Predictions with +/- One Standard Deviation Uncertainty



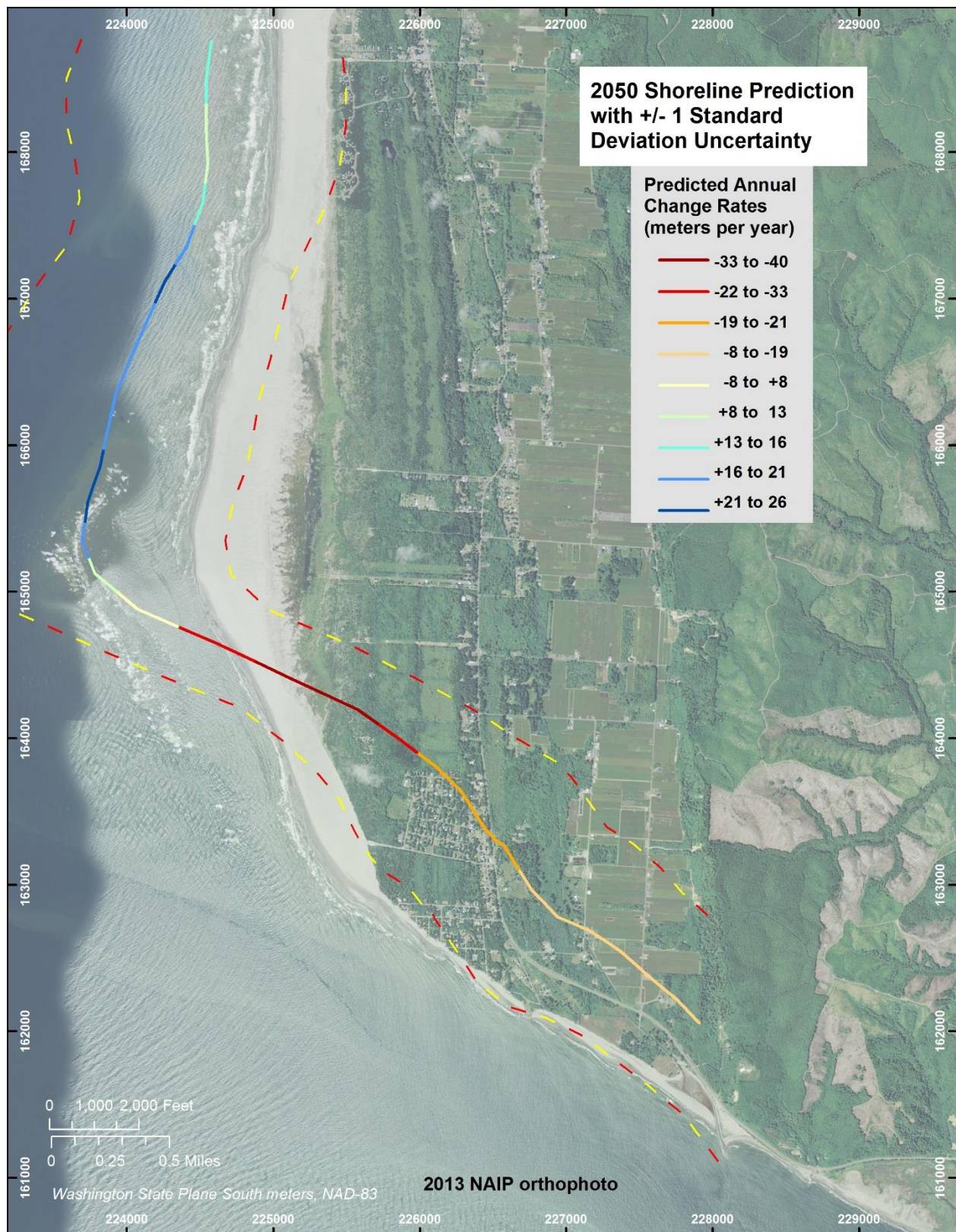
Map showing the predicted 2020 shoreline expressed in terms of shoreline change rate along with uncertainty in position based on +/- one standard deviation (dashed yellow and red lines).



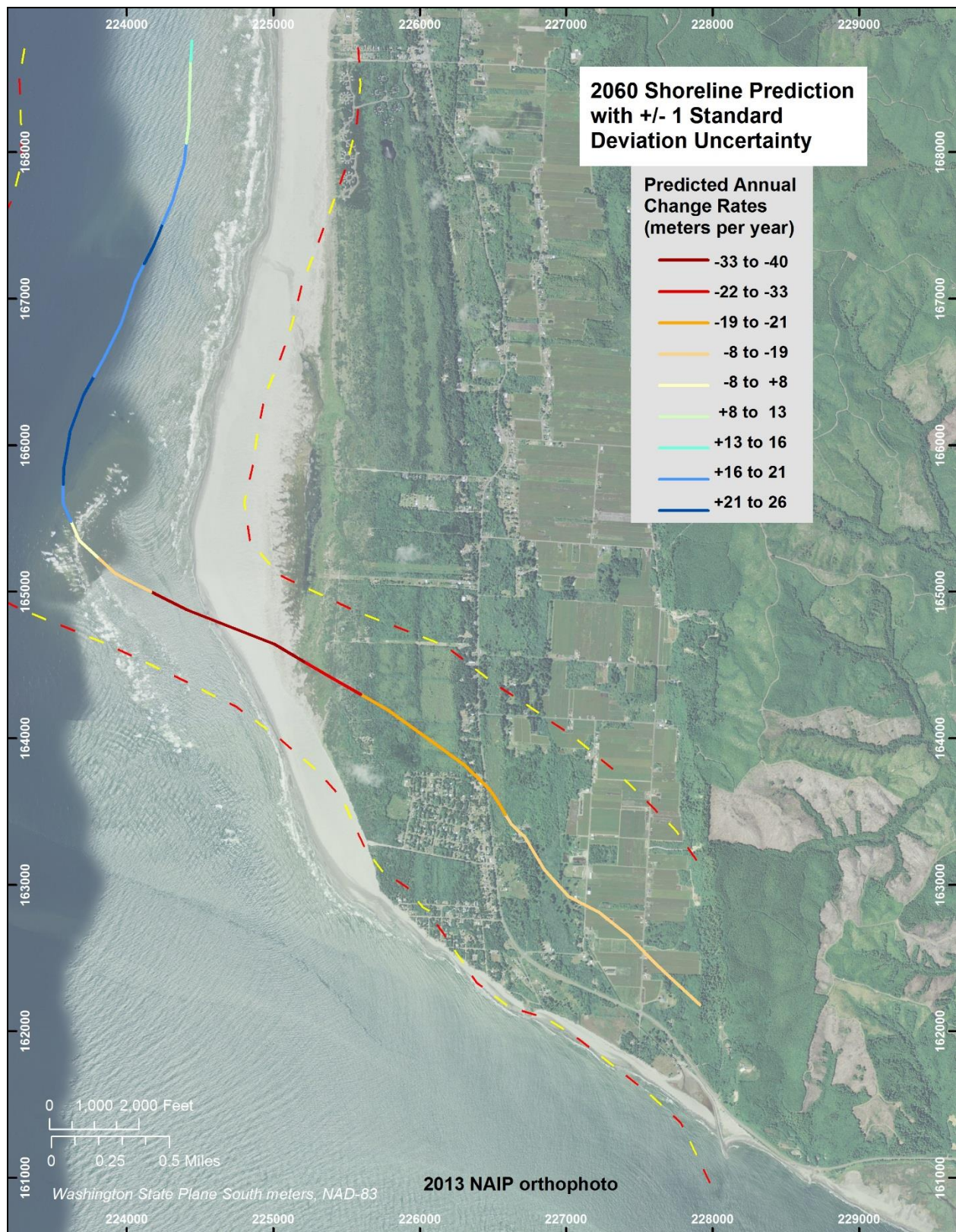
Map showing the predicted 2030 shoreline expressed in terms of shoreline change rate along with uncertainty in position based on +/- one standard deviation (dashed yellow and red lines).



Map showing the predicted 2040 shoreline expressed in terms of shoreline change rate along with uncertainty in position based on +/- one standard deviation (dashed yellow and red lines).



Map showing the predicted 2050 shoreline expressed in terms of shoreline change rate along with uncertainty in position based on +/- one standard deviation (dashed yellow and red lines).



Map showing the predicted 2060 shoreline expressed in terms of shoreline change rate along with uncertainty in position based on +/- one standard deviation (dashed yellow and red line)

-
- ¹ George M. Kaminsky, Peter Ruggiero, Maarten C. Buijsman, Diana McCandless, and Gary Gelfenbaum, (2010). *Historical Evolution of the Columbia River Littoral Cell*. Maine Geology, 273, 1, pages 96–126.
- ² Staff, Pacific County Assessor's Office. Personal Communication, 2014.
- ³ Plot Maps. Provided by the Pacific County Assessor's Office. 2014.
- ⁴ Ibid.
- ⁵ Pacific County, *Washington Comprehensive Plan Update 2010-2030*, (October 2010).
- ⁶ Department of the Army, Corps of Engineers, Seattle District. *Feasibility Report: Navigation and Beach Erosion: Willapa River and Harbor and Naselle River, Washington*, (December 1971).
- ⁷ Pacific County, *Washington Comprehensive Plan Update 2010-2030*, (October 2010).
- ⁸ Department of the Army, Corps of Engineers, Seattle District. *Feasibility Report: Navigation and Beach Erosion: Willapa River and Harbor and Naselle River, Washington*, (December 1971).
- ⁹ Ibid.
- ¹⁰ George M. Kaminsky, et al. (1999). *Mapping Erosion Hazard Areas in Pacific County, Washington*. Journal of Coastal Research, 28, pages 158-170.
- ¹¹ George M. Kaminsky, et al. (2010). *Historical Evolution of the Columbia River Littoral Cell*. Journal of Marine Geology, 273, 1-4, pages 96-126.
- ¹² George M. Kaminsky, et al. (1999). *Mapping Erosion Hazard Areas in Pacific County, Washington*. Journal of Coastal Research, 28, pages 158-170.
- ¹³ Robert A. Holman and Ashbury H. Sallenger Jr. (1986). *High-Energy Nearshore Processes*. Earth & Space Science News, 67, 49, pages 1369-1371.
- ¹⁴ Peter Ruggiero, et al. (2001). *Wave Runup, Extreme Water Levels, and the Erosion of Properties Backing Beaches*. Journal of Coastal Resources, 17, 2, pages 407-419.
- ¹⁵ Hilary F. Stockdon, et al. (2006). *Empirical Parameterization of Setup, Swash, and Runup*. Journal of Coastal Engineering, 53, 7, pages 573-588.
- ¹⁶ Paul D. Komar. (1986). *The 1982-83 El Niño and Erosion on the Coastal of Oregon*. Shore & Beach, 54, pages 3-12.
- ¹⁷ Jonathan C. Allan and Paul D. Komar. (2002). *Extreme Storms on the Pacific Northwest Coast During the 1997-98 El Niño and 1998-99 La Niña*. Journal of Coastal Research, 18, pages 175-193.
- ¹⁸ Peter Ruggiero, et al. (2001). *Wave Runup, Extreme Water Levels, and the Erosion of Properties Backing Beaches*. Journal of Coastal Resources, 17, 2, pages 407-419.
- ¹⁹ Ibid.
- ²⁰ Ashbury H. Sallenger Jr. (2000). *Storm Impact Scale for Barrier Islands*. Journal of Coastal Research. 16, 3, pages 890-895.
- ²¹ Jeremy Mull and Peter Ruggiero. (2014). *Estimating Storm-Induced Erosion and Overtopping Along U.S. West Coast Beaches*. Journal of Coastal Research, 30, 6, pages 1173-1187.
- ²² Peter Ruggiero, et al. (2001). *Wave Runup, Extreme Water Levels, and the Erosion of Properties Backing Beaches*. Journal of Coastal Resources, 17, 2, pages 407-419.
- ²³ Katherine A. Serafin and Peter Ruggiero. (2014). *Simulating Extreme Total Water Levels Using a Time-Dependent, Extreme Value Approach*. Journal of Geophysical Research: Oceans. 119, 9, pages 6305-6329.
- ²⁴ Ashbury H. Sallenger Jr. (2000). *Storm Impact Scale for Barrier Islands*. Journal of Coastal Research. 16, 3, pages 890-895.
- ²⁵ Peter Ruggiero, et al. (2001). *Wave Runup, Extreme Water Levels, and the Erosion of Properties Backing Beaches*. Journal of Coastal Resources, 17, 2, pages 407-419.
- ²⁶ Hilary F. Stockdon, et al. (2007). *A Simple Model for the Spatially-Variable Coastal Response to Hurricanes*. Marine Geology, 238, pages 1-20.
- ²⁷ Peter Ruggiero. (2013). *Is the Intensifying Wave Climate of the U.S. Pacific Northwest Increasing Flooding and Erosion Risk Faster than Sea Level Rise?* Journal of Waterway, Port, Coastal, and Ocean Engineering, 139, 2, pages 88-97.
- ²⁸ Ashbury H. Sallenger Jr. (2000). *Storm Impact Scale for Barrier Islands*. Journal of Coastal Research. 16, 3, pages 890-895.
- ²⁹ Ibid.
- ³⁰ Ibid.